Theoretical Nuclear Physics

DOE/ER/40335--6

DE92 000022

CONTENTS

A. 1991 PROGRESS REPORT - October 1, 1990 to October 1, 1991

1. Consistent RHA-RPA for Finite Nuclei J. R. Shepard, C. E. Price, E. Rost and J. A. McNeil (Colorado School of Mines)

RPA based on the relativistic Hartree approximation (RHA) to finite nuclear ground states. In this latter approach, degrees of freedom associated with the negative energy Dirac sea of nucleons are described via the derivative expansion of the 1-loop effective action. A consistent RPA is obtained by expanding the vacuum-dressed σ- and ω-propagators and retaining only those terms also found in the derivative expansion used for the RHA.

We have additionally examined the influence of 3-momentum cutoffs (or "sideways form-factors") in the Dirac sea on our RHA-RPA calculations. We view such cutoffs as a crude way of suppressing contributions involving small length scales where the finite size of the nucleon almost certainly implies such contributions are unphysical. We find that, when QHD parameters are adjusted to reproduce the saturation point of nuclear matter, the strength of the resulting spin orbit potential for finite nuclei depends strongly on the cutoff momentum. Specifically, a cutoff of *zero* - implying no vacuum contributions – yields the strongest spin orbit interaction while an infinite cutoff corresponding to the standard RHA gives the weakest. A physically plausible 3-momentum cutoff equalling $2M_{proton}$ provides a good description of, *e.g.*, the $0d_{5/2}$ versus $0d_{3/2}$ splitting in ^{40}Ca.

Our RPA results show the importance of the consistency mentioned above. For example, the calculated (e,e') Coulomb form factors for the lowest 3^- levels in ^{16}O and ^{40}Ca display the high degree of collectivity seen in the data only in the consistent calculations. Using a simple local density approximation in the RHA ground state and the full σ- and ω-propagators in the RPA diminish the peak values of the form factors by at least a factor of two.

For the quasielastic (e,e') Coulomb response, consistency *per se* is not so important as it is for the low-lying collective excitations. However, as also noted by, *e.g.*, Horowitz and Piekarewicz,[1] inclusion of vacuum contributions appreciably improves the agreement between theory and experiment for ^{12}C and ^{40}Ca at $\mid \vec{q} \mid$=400 and 550 MeV/c.

A preliminary report of this work has appeared in Ref. 2 and a manuscript to be submitted to Physical Review **C** is in preparation.

1. C. J. Horowitz and J. Piekarewicz, Nucl. Phys. **A511** 461 (1990)
2. J. R. Shepard in "From Fundamental Fields to Nuclear Phenomena", C. E. Price and J. A. McNeil, eds., (World Scientific, Singapore) 1991, pp. 190-211

2. **Exact Vacuum Polarization in Finite Nuclei** T.C. Ferrée and J.R. Shepard

In QHD nuclear structure calculations for symmetric, closed-shell systems, the nucleus is viewed approximately as a system of point nucleons interacting through the exchange of isoscalar mesons. These mesons can produce virtual particle-antiparticle pair excitations of the vacuum in a process called vacuum polarization. These virtual pairs interact with the on-shell valence nucleons as well as with each other, and may significantly influence the properties of the many-body system.

Calculating the effects of vacuum polarization in a finite system of nucleons poses a challenging computational problem. One must deal with contributions from an infinite number of negative energy states in the Dirac sea. In a renormalizable field theory like QHD-I,[1] divergent vacuum contributions are regularized to obtain finite expressions which do not depend upon cutoffs imposed during the regularization. However, even with the renormalization procedure well-understood, there are numerical difficulties which must be overcome in dealing with an infinite number of nucleon eigenstates in a finite nucleus.

Several authors have addressed this problem, beginning with Chin,[2] who calculated the effects of vacuum polarization in uniform nuclear matter using the Hartree 1-Loop Expansion[1] to obtain self-consistent solutions. Horowitz and Serot[3] then applied this result to finite nuclei by taking the vacuum contributions at each point in the nuclear interior to be equal to those in the infinite system, but given by the value of the local scalar field at that point. Perry improved upon this Local Density Approximation (LDA) by introducing the Derivative Expansion (DE).[4] He showed that an expansion in inverse powers of the effective nucleon mass is also an expansion in powers of derivatives of the potentials, the first term of which is the LDA result. This expansion appears to converge in QHD-I, and provides a good method for approximating the effects of the Dirac sea. While Perry only carried these calculations to first order in the Hartree 1-Loop Expansion, Wasson[5] later used this method self-consistently to study vacuum polarization in finite nuclei.

In all of these methods, the vacuum is included in such a way that one need only calculate individual eigenstates for the valence nucleons, and not the infinite number of negative energy eigenstates in the Dirac sea. In calculating a few bound states, a Numerov or Runge-Kutta integration scheme is adequate, and the results are relatively insensitive to the boundary conditions being imposed outside the nucleus. However, including the effects of vacuum polarization exactly requires not only a method for calculating bound and continuum negative energy states exactly, but forces one to consider carefully the boundary conditions being imposed.

Recently, Blunden[6] showed that the effects of vacuum polarization can be included exactly by integrating the nonspectral form of the Dirac single-particle Green's function along the imaginary frequency axis. Since the Green's function has no poles along this axis, the integral is well-behaved, and with a simple extrapolation it converges to agree well with the DE results. His calculations were performed in 1+1 dimensions using Gaussian vector and scalar potentials, but without the self-consistency inherent in the Hartree 1-Loop Expansion. In addition, he derived finite renormalization counterterms involving second derivatives of the potentials, but did so using a questionable expansion of the exact Hartree Green's function. More recently, Wasson and Koonin[7] derived an extrapolation procedure based on the WKB approximation which is applicable to both spectral and nonspectral methods. This procedure was investigated in several cases

with self-interacting scalar fields, and is shown to significantly improve convergence in the Dirac sea.

We have calculated the effects of vacuum polarization exactly at the 1-Loop level in a 1+1 dimensional finite system of Dirac nucleons, employing self-consistent vector and scalar potentials. We impose periodic boundary conditions with a period large on the scale of the nucleus, the motivation being that for the deep negative energy states this is the natural choice to describe slightly perturbed plane waves. These boundary conditions have the effect of discretizing the spectrum of unbound states, allowing each state to be labeled by its nodes and parity.

In calculating the effects of the entire Dirac sea, a Numerov or Runge-Kutta integration scheme is clearly inadequate on its own, since the maximum number of nodes is restricted by the number of grid points chosen for the integration. In fact, the number of grid points must be at least an order of magnitude greater than the number of nodes of the deepest state considered, or the high energy part of the spectrum will be sensitive to the grid. On the other hand, one cannot choose an arbitrarily fine grid because of machine error and constraints in computing time. Thus it is essentially impossible to reach convergence in the Dirac sea by Numerov or Runge-Kutta methods alone. While one may derive an extrapolation procedure for deep negative energy states based on the Eikonal approximation, we have seen that the presence of a vector potential leads to a nonzero baryon density in the exterior of the nucleus which renders the solution highly unstable. An inconsistency in this Numerov/Eikonal approach is apparent when one considers the spectrum of eigenvalues obtained by the two methods. For any number of grid points chosen, there are very few states where the two spectra agree to high precision, even at energies where the Eikonal approximation is thought to be valid. It seems that one cannot construct a well-behaved basis of eigenfunctions from the union of these two methods.

A better method is to diagonalize the Dirac hamiltonian in a finite basis of free eigenstates, which in 1+1 dimensions amounts to a Fourier decomposition of the exact eigenstates. (A similar diagonalization method has been used previously by Kahana and Ripka[8] in 1+3 dimensional calculations of finite solitons.) The basis obtained is complete within the finite space which it defines, and does not have the instability problems which are present in the Numerov/Eikonal approach. The stability of the method is traceable to the fact that the free basis consists of sines and cosines which satisfy $\sin^2 x + \cos^2 x = 1$ independent of argument. This, together with the orthogonality of the eigenvectors which can easily be realized numerically to very high precision, ensures *unrenormalized* vacuum densities which are well-behaved even when the negative energy states are affected by strong potentials. This in turn yields reliable *renormalized* vacuum densities in spite of enormous cancellations. Contributions from the rest of the Dirac sea may then be approximated using the LDA results. The finite basis is chosen large enough so that self-consistent solutions are insensitive to small changes in its size, which requires fewer than a hundred states in the Dirac sea to be calculated by diagonalization. Without the LDA results appended to the finite basis contributions, many more states would be required to achieve convergence, if one uses the same coupling constants in both cases.

Lastly, we have determined how to derive the finite renormalization counterterms appropriate to our periodic boundary conditions. These are obtained by considering small deviations from the uniform system in momentum space, and identifying terms proportional to the spatial momentum transfer squared with second derivatives of the potentials. Although in 1+1 dimensions these make finite contributions to the nucleon energy and meson source densities, and are therefore not part of the regularization of these quantities required to remove divergences, they are required to renormalize the

polarization insertions so that they and their first derivatives with respect to q^2 vanish at $q^2 = 0$ and $m^* = m$.

Work is in progress to study the effects of vacuum polarization when treated via the exact Fourier/LDA method, and to compare these results with the results obtained via the various approximations already discussed. In particular, it remains to be seen if Blunden's nonspectral approach and our Fourier/LDA approach give similar results when considering contributions from the entire Dirac sea. Also, one may ask if it is appropriate to consider contributions from the entire Dirac sea. It is possible to obtain coupling constants by imposing a three momentum cutoff in the Dirac sea of the infinite system at saturation, and then use these coupling constants in the finite system while including contributions from only that part of the Dirac sea included within the cutoff. An immediate extension of this work is to explore the effects of vacuum polarization on the normal mode (RPA) excitations of finite nuclei, and we will consider these effects after the ground state problem is well understood.

1. B.D. Serot and J.D. Walecka, Adv. Nucl. Phys. **16** 35 (1986)
2. S.A. Chin, Ann. Phys. (N.Y.) **101** 301 (1977)
3. C.J. Horowitz and B.D. Serot, Phys. Lett. **140B** 181 (1984)
4. R.J. Perry, Phys. Lett. **182B** 269 (1986)
5. D.A. Wasson, Phys. Lett. **210B** 41 (1988)
6. P.G. Blunden, Phys. Rev. **C41** 1851 (1990)
7. D.A. Wasson and S.E. Koonin, Phys. Rev. **D43** 3400 (1991)
8. S. Kahana and G. Ripka, Nucl. Phys. **429A** 462 (1984)

3. Isovector Correlations in QHD Description of Nuclear Matter J. R. Shepard and C. J. Horowitz (Indiana University)

Isoscalar (T=0) correlations induced in nuclear matter by σ- and ω- meson exchange have been well-studied in the context of the QHD model of nuclear dynamics. Such correlations play crucial roles in, *e.g.*, the description of isoscalar magnetic moments[1] and suppression of the Coulomb sum in (e,e') quasi-elastic scattering.[2] Isovector (T=1) correlations generated by π- and ρ-meson exchange are much less thoroughly investigated. Recent experiments[3] at the Neutron-Time-of-Flight (NTOF) facility at LAMPF have sought signatures of such correlations in the spin observables of the quasi-elastic (p,n) reaction on ^{12}C and ^{40}Ca. Preliminary results suggest no difference between the relative strengths of the longitudinal-vs-transverse spin responses in nuclei as compared to those observed on deuterium. That is, nuclear correlations appear to have no influence on relative longitudinal-vs-transverse T=1 responses. This is surprising in light of the (naive) expectation that the attractive π-interaction should significantly *soften* the longitudinal spin response while the repulsive ρ-interaction should *harden* the transverse. We have undertaken a study of π- and ρ- correlations in nuclear matter using an RPA approach based on QHD-MFT.[4] Here properties of the nuclear ground state depend on the mean fields of isoscalar σ- and ω-mesons which help determine the nucleon propagator, $G(p)$. Our π- and ρ- interactions are based on the following NN vertices:

$$\pi\mathrm{NN}: \qquad g_\pi \frac{\not{q}\gamma^5}{2M}\vec{\pi}\cdot\vec{\tau}$$

$$\rho\mathrm{NN}: \qquad \frac{-ig_\rho}{2}\left[\gamma^\mu + \frac{iC_\rho}{2M}\sigma^{\mu\nu}q_\nu\right]\vec{P}_\mu\cdot\vec{\tau}$$

where $\vec{\pi}(\vec{P})$ is the $\pi-(\rho-)$ field. The results reported here employ coupling constants from Ref. 5. The presence of derivative contributions in the πNN vertex and the tensor term of the ρNN vertex imply "contact terms" for interactions involving two such vertices. These zero-ranged interactions are expected to be suppressed both in free space and in nuclear matter by short-ranged correlations induced by the hard-core of the NN interaction. We account for such suppression phenomenologically by modifying the relevant meson propagators as follows:

$$D_0 = \frac{1}{q^2-\mu^2} \;\rightarrow\; D_0(g') = \frac{1}{q^2-\mu^2} - \frac{g'}{q^2}$$

where μ is the meson mass and g' is a free parameter. Note that $g'=1$ corresponds to *total* suppression of the contact term.

Solution of the RPA equations and calculation of various responses is straightforward:

$$\Pi_{RPA} = \Pi_0 + \Pi_0 D_0(g')\Pi_{RPA}$$

$$S_\theta(\omega) = -\frac{1}{\pi}\mathrm{Im\ Tr}\left[\theta\ \Pi(\omega)\ \theta\right]$$

Here we focus on the pionic response, $S_\pi(\omega)$, for which

$$\theta \rightarrow g_\pi \frac{\not{q}\gamma^5}{2M}\tau_z$$

and on the ρ-response, $S_\rho(\omega)$, where

$$\theta \rightarrow \frac{-ig_\rho}{2}[\gamma^\mu + \frac{iC_\rho}{2M}\sigma^{\mu\nu}q_\nu].$$

We also compute the transverse electromagnetic response, $S_T(\omega)$, where

$$\theta \rightarrow J^1_{em}$$

with

$$J^\mu_{em} = \frac{1}{2}(1+\tau_z)\gamma^\mu + \frac{i}{2M}(\kappa_0 + \kappa_1\tau_z)\sigma^{\mu\nu}q_\nu$$

where $\kappa_0 = -0.06$ and $\kappa_1 = 1.85$ are the T=0 and T=1 anomalous moments of the nucleon, respectively. Note that, while explicit reference to nucleon form factors has been omitted in describing J^μ_{em}, our calculations in fact employ the form factors of Ref. 6.

A brief summary of our preliminary results begins with an examination of the π-response at $\mid \vec{q} \mid = 350$ MeV/c which appears in Figure 1. As indicated by the solid line, the correlated π- response for $m^* = m$ and $g'_\pi = 0$ shows enormous attractive collectivity indicative of the nearness of π-condensation for these parameters. (See, *e.g.*, Ref. 7) Clearly, such parameters are unphysical and we focus on quantities related to the quasi-elastic $(\vec{p},\vec{n})$ measurements mentioned above. For example, the "super-ratio" of the separated longitudinal-vs-transverse-spin responses has been extracted. In the plane-wave limit and subject to a few other reasonable assumptions, this super-ratio is related to the responses described above via

$$R_{LT} \equiv \frac{(S_L/S_T)_{\text{nucleus}}}{(S_L/S_T)_{\text{deuterium}}} \leftrightarrow \frac{(S_\pi/S_\rho)_{RPA}}{(S_\pi/S_\rho)_{MFT}}$$

where the MFT responses omit correlations and assume $m^* = m$. In Figs. 1 and 2 (the π- and ρ-responses, respectively) all calculations were performed using $k_F = 1fm^{-1}$ and the RPA results are for $m^*/m = 0.85$. These latter quantities are roughly appropriate to the average nuclear density at which the 500 MeV quasi-elastic (p,n) process occurs on ^{40}Ca (note that for (e,e') processes where the entire nuclear volume is sampled, $k_F = 1.16fm^{-1}$ and $m^*/m = 0.73$ is appropriate). Fig. 1 shows that RPA correlations at $m^* = m$ are greatly suppressed by $g'_\pi \rightarrow 0.8$. Nevertheless, some slight attractive collectivity remains, consistent with non-relativistic analyses.[9]

A similar set of calculations for the ρ-response appears in Fig. 2 where, with $g'_\rho = 0$ and $m^* = m$, RPA correlations display weak attractive collectivity. Using $g'_\rho = 0.6$ results in slightly stronger *repulsive* correlations which reduce the overall response and shift it to somewhat higher ω. The overall result is that RPA and g' effects give a super-ratio R_{LT} significantly larger than one and again familiar from non-relativistic treatments.

We now examine the influence of $m^*/m < 1$ on the responses and R_{LT}. Small values of m^* tend to reduce the strength of vertices with derivative coupling and those effects are seen clearly in the $m^*/m = 0.85$ π- and ρ- responses. Fig. 1 shows that the m^* effect reduces S_π by more than 25%, while a somewhat smaller reduction of the ρ-response is evident in Fig. 2 These reductions have no counterparts in non-relativistic treatments, but in fact, together with the RPA and g' effects, yield a super-ratio very near unity and quite similar to the experimental values. More thorough analyses are in progress, but initial indications are that the m^* effect may be crucial in understanding the observed isovector spin responses.

To provide a means of assessing the physical content of our calculations, we compare our transverse and Coulomb (e, e') responses with the Scalay data[10] for ^{40}Ca at $\mid \vec{q} \mid =$ 410 MeV in Figs. 3 and 4. Both MFT (dashed curves) and full RPA results (solid curves) are shown. These calculations employ $k_F = 1 fm^{-1}$ and $m^*/m = 0.73$ as well as $g'_\rho = 0.6$.

1. See, *e.g.*, J.R. Shepard, E. Rost, C.-Y. Cheung, and J.A. McNeil, Phys. Rev. **C37** 1130 (1988) and references contained therein.
2.) See, *e.g.*, J.P. Chen *et al.*, Phys. Rev. Lett. **66** 1283 (1991) and references contained therein.
3. X.Y. Chen, private communication, 1991 C.U. Experimental Nuclear Physics Progress Report, and to be published.
4. B.D. Serot and J.D. Walecka, Adv. Nucl. Phys. **16** 1 (1986)
5. R. Machleidt in "Relativistic Dynamics and Quark-Nuclear Physics," Mikkel B. Johnson and Alan Picklesimer, eds., John Wiley and Sons, NY, 1986
6. Shigeru Nishizaki, Haruki Kurosawa and Toshio Suzuki, Phys. Lett. **171B**, 1 (1986)
7. J.D. Dawson and J. Piekarewicz, SCRI preprint, January 1991 and to be published.
8. J.R. Shepard, E. Rost and J.A. McNeil, Phys. Rev. **C33** 634 (1986)
9. See, *e.g.*, H. Esbensen, H. Toki, and G.F. Bertsch, Phys. Rev. **C31** 1816 (1985)
10. Z.E. Meziani *et.al.*, Phys. Rev. Lett. **52** 2130 (1984)

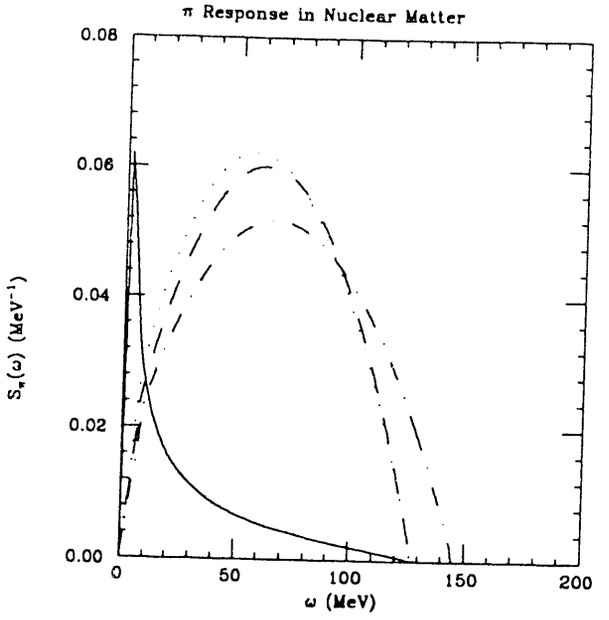

Fig. 1 The π-response/nucleon in nuclear matter using $k_F = 1.0$ and $m^*/m = 0.85$ as well as $g'_\pi = 0.80$

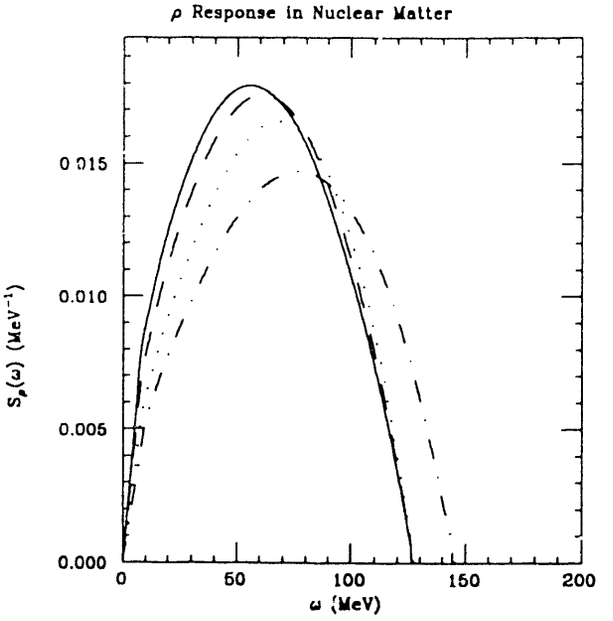

Fig. 2 The π-response/nucleon in nuclear matter using $k_F = 1.0$ and $m^*/m = 0.85$ as well as $g'_\rho = 0.60$.

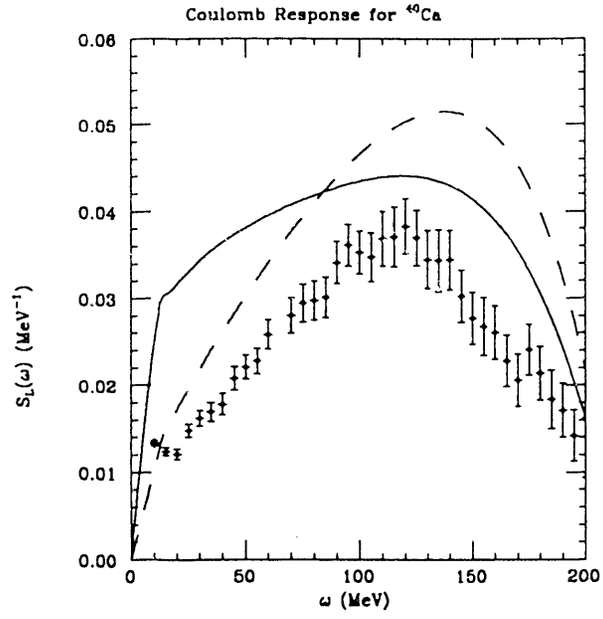

Fig. 3 The (e, e') Coulomb response for ^{40}Ca using $k_F = 1.16$ and $m^*/m = 0.73$ as well as $g'_\rho = 0.60$.

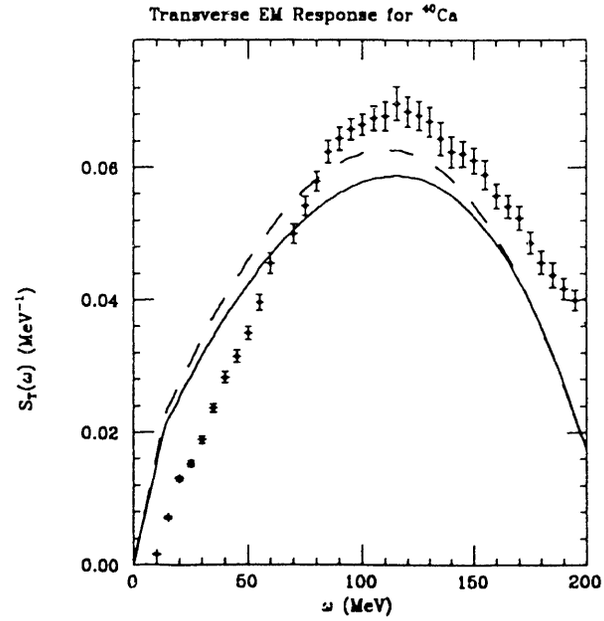

Fig. 4 The transverse (e, e') response for ^{40}Ca using $k_F = 1.16$ and $m^*/m = 0.73$ as well as $g'_\rho = 0.60$.

4. Nuclear Response Functions in Quasielastic Electron Scattering, E. Rost

We have been actively involved for several years in a program to study quasielastic responses in finite nuclei. High quality data are now available from electron scattering experiments where the longitudinal and transverse response functions, $S_L(\mathbf{q},\omega)$ and $S_T(\mathbf{q},\omega)$, have been measured. These quantities represent form factors that measure the response of the nucleus to electromagnetic probes

$$\begin{aligned} S_L(\mathbf{q},\omega) &= \sum_n \delta(\omega-\omega_n)\Big|\langle\Psi_n|\rho(q)|\Psi_0\rangle\Big|^2 \\ S_T(\mathbf{q},\omega) &= \sum_n \delta(\omega-\omega_n)\Big|\langle\Psi_n|J_\lambda(q)|\Psi_0\rangle\Big|^2 \end{aligned} \tag{1}$$

where ρ and J_λ ($\lambda = \pm 1$) are the nuclear charge and current operators and Ψ_n is a nuclear excited state wavefunction with excitation energy ω_n.

It is convenient[1] to write the response functions in terms of a many-body operator, the polarization tensor, defined by the time-ordered product

$$i\Pi^{\mu\nu}(x,y) = \langle\Psi_0|T\big[J^\mu(x)J^\nu(y)\big]|\Psi_0\rangle. \tag{2}$$

The polarization tensor is evaluated in the Hartree approximation and after some manipulation[2] is expressed in terms of non-spectral, mean-field Green functions

$$\begin{aligned} -i\Pi^{ij;k\ell}_{MF}(\mathbf{x},\mathbf{y},\omega) = \sum_h \big[&\psi^i_h(\mathbf{x})\bar\psi^\ell_h(\mathbf{y})G^{kj}_{MF}(\mathbf{y},\mathbf{x};\epsilon_h-\omega) \\ &+ G^{i\ell}_{MF}(\mathbf{x},\mathbf{y};\epsilon_h+\omega)\psi^k_h(\mathbf{y})\bar\psi^j_h(\mathbf{y})\big] \end{aligned} \tag{3}$$

where the sum is over occupied hole states, h, with wavefunction ψ_h and i,j,k,ℓ are Dirac indices.

The non-spectral Green functions are obtained in a method we have developed[2] by solving the inhomogeneous Dirac equation in configuration space

$$\big[\omega\gamma^0 + i\gamma\cdot\nabla - M - \Sigma_{MF}(\mathbf{x},\mathbf{y};\omega)\big]G_{MF}(\mathbf{x},\mathbf{y};\omega) = \delta(\mathbf{x}-\mathbf{y}) \tag{4}$$

in the presence of the self-consistent mean field, Σ_{MF}, and with the same boundary conditions satisfied by the free propagator.

It is not difficult to generalize the mean field propagator of Eq. (3) to include particle-hole correlations in the random phase approximation (RPA) method. Schematically, one replaces Π_{MF} in Eq. (3) by the solution to the integral equation

$$\Pi_{RPA} = \Pi_{MF} + \Pi_{MF}\ \mathcal{K}\ \Pi_{RPA} \tag{5}$$

where $\mathcal{K}$ is the RPA kernel (see ref. 2 for details.) We solve Eq. (5) numerically on a grid in configuration space.

Explicit formulas for the response functions, S_L and S_T, follow[3] after expanding in vector spherical harmonics and separating isoscalar and isovector contributions. The isospin separation allows us to make a convenient approximation that saves considerable computation. The electromagnetic current operator for isospin t is

$$J^{\mu}_{t}(q) = F_1(q^2)\gamma^{\mu} + F_2(q^2)\frac{i\kappa_t}{2M}\sigma^{\mu\nu}q_{\nu} \tag{6}$$

where the anomalous moments are $\kappa_0 = -0.06$ and $\kappa_1 = +1.85$ for isoscalar and isovector currents. Hence we ignore the isoscalar anomalous terms. The isovector anomalous terms are substantial; however they are relatively insensitive to RPA correlations so we simply use the mean-field polarization tensor, Π_{MF}, in computing their contributions to S_T. Even with these approximations, the calculation of S_L and S_T for finite nuclei requires considerable numerical effort.

Figure 1 shows results for a ^{12}C target at a momentum transfer of 400 MeV/c. The RPA calculations are nearly identical to those of ref. 3 although our numerical techniques are considerably different. The RPA calculations give a reasonable representation of the data near the quasi-elastic peaks—more details are found in ref. 4. The behavior of S_T at high q is not at all described by the RPA theory and it is believed that other physics (e.g., Δ isobars) is responsible. We have studied this region with our DRPA code in order to see if it is possible to obtain some insight without resort to other degrees of freedom. In particular retardation causes a complex folding at $\omega > m_{\pi}$ in the evaluation of $\mathcal{K}$ in Eq. (5). Unfortunately we are not able to find any effects so enormous as to give a rising S_T at high ω.

Finally we have been investigating the very recent high-ω (e,e′) data[5] taken at SLAC using an ^{56}Fe target. We have extended the DRPA code to handle this extreme case (35 J values were required.) The data, if correct, are very interesting. We note that nuclear matter calculations[6] and finite nucleus RPA calculations[3] yield curves where *S_L and S_T are roughly proportional* whereas the data at high ω differ greatly. We plan to study this case more closely in order to see what the finite nucleus effects are and to see if we can understand what features in our model are needed in order to change the shape of the transverse response relative to the longitudinal response.

1. A.L. Fetter and J.D. Walecka, *Quantum Theory of Many-Body Systems*, (McGraw-Hill, New York, 1971)
2. J.R. Shepard, E. Rost and J.A. McNeil, Phys. Rev. C **40** 2320 (1989)
3. C.J. Horowitz and J. Piekarewicz, Nucl. Phys. **A511** 461 (1990)
4. J.R. Shepard in *Proceedings of the Workshop: From Fundamental Fields to Nuclear Phenomena*, eds. J.A. McNeil and C.E. Price, (World Scientific, 1991), p. 190
5. J.P. Chen *et al.*, Phys. Rev. Lett. **66** 1283 (1991)

6. J.W. Van Orden, Ph.D. thesis, Stanford University, 1978
7. P. Barreau *et al.*, Nucl. Phys. **A402** 515 (1983)

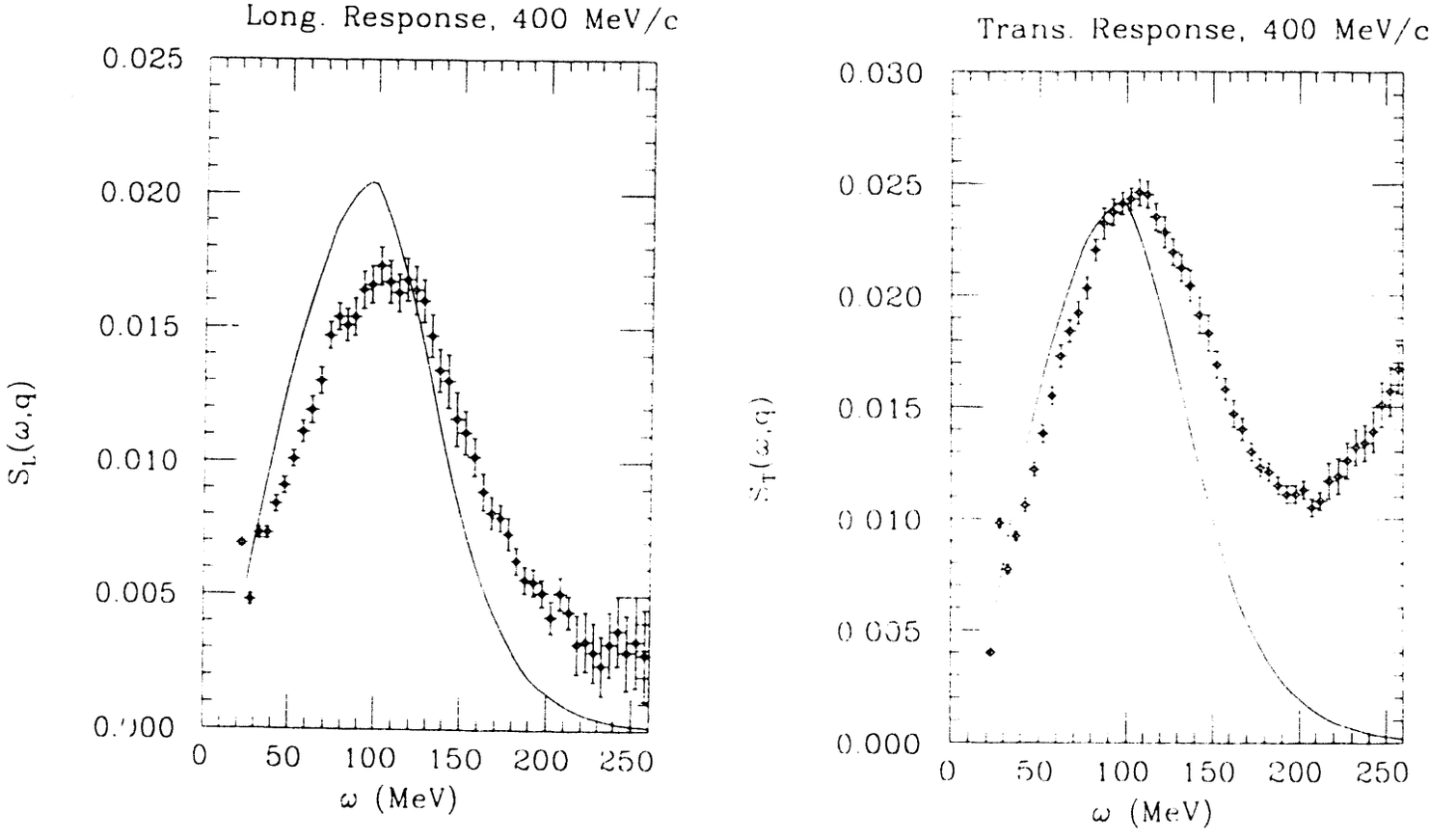

Fig. 1. Longitudinal and transverse response functions for ^{12}C at q = 400 MeV/c. The solid line is the result of a RPA calculation including vacuum polarization effects and is in close agreement with the calculation of ref. 3. Experimental data were obtained from ref. 7.

5. Charge Density Differences for Nuclei Near ^{208}Pb in Quantum Hadro-Dynamics

C. E. Price and R. J. Furnstahl (University of Maryland)

There is recent data[1,2] on the charge densities of various nuclei near ^{208}Pb (*e.g.* ^{206}Pb, ^{205}Tl and ^{204}Hg). The difference between the charge densities of two such nuclei that differ by one or two protons should be dominated by the charge density associated with the last occupied proton orbital. For these nuclei near ^{208}Pb, the last occupied proton state is the 3s1/2 orbital, which has a characteristic two node shape with a large central maximum. This shape should provide a unique signature for the effects of this orbital in the charge density difference, and should make it possible to identify any deviations from the pure single particle picture.

There are two effects that are expected to cause the charge density difference to deviate from the pure 3s1/2 shape. First, the removal of even a single proton will induce some polarization in the remaining core orbitals so that the charge densities of the cores of two neighboring nuclei (like ^{205}Tl and ^{206}Pb) will not cancel exactly. Secondly, the occupation numbers of the least bound proton orbitals need not be identical for these heavy nuclei. For example, rather than being dominated by the removal of a single proton (or pair of protons) from the 3s1/2 orbital, the charge density difference may be primarily due to the removal of a "fraction" of a proton from each of the 3s1/2 and 2d3/2 orbitals (or any more complicated fractional level occupation schemes).

In this work, we study the charge densities of ^{206}Pb, ^{205}Tl and ^{204}Hg in the context of quantum hadro-dynamics[3] (QHD). This model has been very successful in describing a wide range of nuclear ground state properties throughout the periodic table, and typically provides agreement with experiment that is on the same level as that obtained with a non-relativistic Skyrme model.[4] For these calculations, we have used both linear (L) and nonlinear (NL) parametrizations of QHD.

A particularly clean isolation of the 3s1/2 contribution can be obtained by converting the charge density measurements into a ratio of cross sections as a function of momentum transfer. Figures 1 and CSH show the cross section ratios for ^{205}Tl/^{206}Pband ^{204}Hg/^{206}Pb respectively. in both figures the solid curve is the experimental (obtained form a Fourier-Bessel fit to the charge density data) and the dashed (dashed-dotted) curve is the calculation using the linear (non-linear) parameterization of QHD and obtained by using the DWBA code HADES[5] to calculate the cross section ratios from the calculated coordinate space charge densities. For these ratios , the contribution of the 3s1/2 state is characterized by the large peak near 2 fm^{-1}, which is evident in both the experimental results and the calculations. Both the dominant peak and the overall scale of the structure is significantly enhanced in the calculations compared to the experimental results (although the experimental error bars, not shown, are fairly large).

The calculations shown in figs. 1 and 2, are very similar to those obtained from non-relativistic Hartree-Fock calculations using phenomenological effective interactions (see ref. 1 for ^{205}Tl and ref. 2 for ^{204}Hg). In these earlier calculations core polarization played an important role but fractional level occupancies were needed to describe the data.

In order to understand the discrepancy between our calculations and experiment, we likewise consider the effects of fractional level occupancy. Since we are only interested

in the cross section *ratios*, it is sufficient to leave the level filling of ^{206}Pb fixed and only vary the occupancy of the least bound levels in either ^{205}Tl or ^{204}Hg. In figs. 1 and 2, we show the cross section ratios for ^{206}Pb - ^{205}Tl and ^{206}Pb - ^{204}Hg obtained by varying the occupancy of the high lying proton orbitals (dotted curves). For these calculations, we have assumed that the neutron occupancies are not affected and that the changes in the proton occupancies are restricted to the 3s1/2 and 2d1/2 shells.

For ^{206}Pb - ^{205}Tl, we used the occupancies suggested by Frois's[1] comparison of the experimental results with the mean-field calculations of Campi *et al.*[6] Specifically, there are 0.7 protons removed from the 3s shell and 0.3 protons removed from the 2d shell. This level occupancy is minimally sufficient to bring our QHD results into agreement with the experimental density. Our dominant peak near 2 fm^{-1} is still a bit too large and the overall structure remains slightly enhanced. The agreement could be improved by using occupancies of 0.6 and 0.4 for the 3s and 2d levels respectively. This larger 3s occupancy is supported by the theoretical calculation of Pandharipande *et al.*[7] in which the occupation probabilities of shell-model orbits in the lead region are estimated by the addition of random-phase approximation corrections to nuclear matter results.

For ^{206}Pb - ^{204}Hg, we have used the occupancies suggested in ref. 2, based on the average of the occupation numbers required to bring three separate non-relativistic calculations into agreement with experiment. Namely, $\sim$ 1.0 proton removed from the 3s orbital and $\sim$ 1.0 proton removed from the 2d orbital (this corresponds to a fractional occupancy of .5 for each of the 3s1/2 levels). Again this occupancy is sufficient to bring our results into minimal agreement with experiment, but the agreement could be improved by removing slightly fewer protons from the 3s level. Since the three calculations of ref. 2 had a spread of about $\pm$10%, such a reduction would still be consistent with the non-relativistic calculations. It is important to point out that, particularly for an even-even nucleus like ^{204}Hg, the fractional occupation of the levels near the Fermi surface should be included via the pairing approximation as has been used by Ring *et al.*[8] rather than by the simple occupation number variation that we have employed here. While it is not expected that the pairing effects would alter the qualitative features of our results, it is likely that the simple picture of the charge density difference in terms of only two levels (the 3s and 2d) would be changed.

1. B. Frois, J. M. Cavedon, D. Goutte, M. Huet, Ph. Leconte, C. N. Papanicolas, X.-H. Phan, S. K. Platchkov, S. E. Williams, W. Boeglin and I. Sick, Nucl. Phys. **A396** 409c (1983).
2. A. Burghardt, PhD Thesis, University of Amsterdam.
3. B. D. Serot and J. D. Walecka, Adv. in Nucl. Phys. **16** (Plenum, New York, 1986).
4. C. J. Horowitz and B. D. Serot, Nucl. Phys. **A368** (1981) 503; S. J. Lee *et al.*, Phys. Rev. Lett. **57**, 2916 (1986); **59**, 1171 (1987); C. E. Price and G. E. Walker, Phys. Rev. **C36**, 354 (1987); W. Pannert, P. Ring, and J. Boguta, Phys. Rev. Lett. **59** (1987) 2420; R. J. Furnstahl, C. E. Price, and G. E. Walker, Phys. Rev. **C36** (1987) 2590; U. Hofmann and P. Ring, Phys. Lett. **214B** 307 (1988).
5. J. Kelly, private communication
6. X. Campi and D. W. L. Sprung, Nucl. Phys. **A194** 401 (1972).

7. V. R. Pandharipande, C. N. Papanicolas and J. Wambach, Phys. Rev. Lett. **53** 1133 (1984).
8. Y. K. Gambhir and P. Ring, Phys. Lett. **B202** 5 (1988) and references therein.

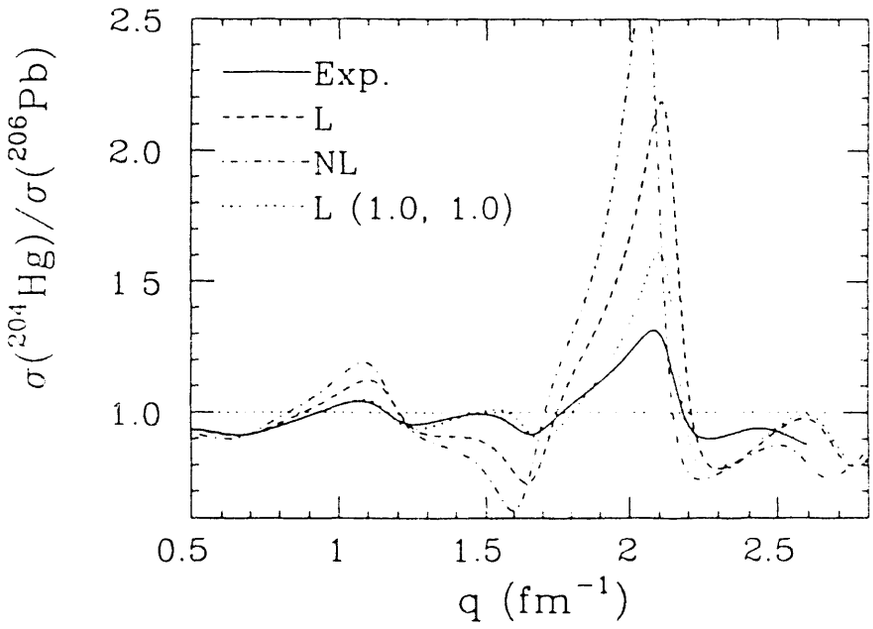

Fig. 1. Cross section ratio for ^{206}Pb – ^{205}Tl. The solid line is the experimental result, the dashed line is from the linear QHD model, the dashed-dotted line is from the nonlinear version of QHD, and the dotted line includes fractional level occupancies.

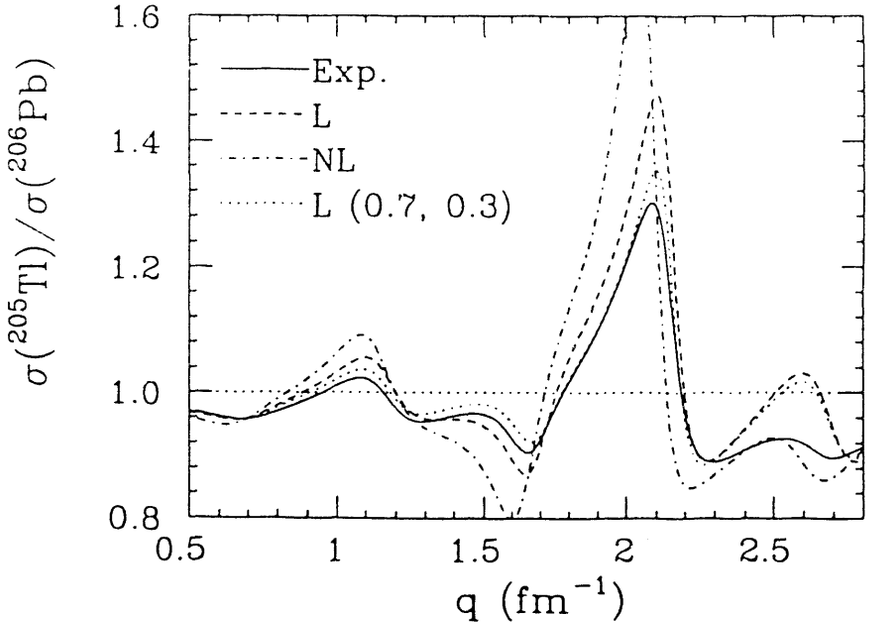

Fig. 2. Cross section ratio for ^{206}Pb – ^{204}Hg. The curves are as described in figure 1.

6. Excitation of the 10.957 MeV 0^-; T=0 State in ^{16}O by 400 MeV Protons

E. Rost (with J. King and TRIUMF-Toronto group)

The measurement of inelastic proton-nucleus spin observables provides details of the nucleon-nucleus interaction that are not otherwise available. The $0^+ \rightarrow 0^-$ transition is especially interesting since it requires a spin-flip in the interaction. Since only J=0 states are involved, complexities due to nuclear structure and the nuclear interaction should be greatly reduced. In a non-relativistic impulse approximation, the direct part of the interaction vanishes under time reversal invariance while the exchange part does not[1], resulting in the relations

$$P = -A_y, \qquad D = -1, \qquad A = R', \qquad R = -A'$$

for the Wolfenstein parameters. An additional simplification in the interaction occurs since the spin-orbit component is zero while the central component is very weak[2]. Thus a measurement of the cross section and analyzing power for the $0^+ \rightarrow 0^-$ transition should allow for identification of the tensor-exchange part of the nucleon-nucleus interaction. A relativistic impulse approximation calculation, on the other hand, predicts a non-zero value for A_y without the explicit inclusion of exchange.[3] This is accomplished through coupling between upper and lower components of Dirac spinors. A relativistic model (DREX) including explicit exchange is also available[4].

The results reported in this work are from a program to measure the cross section and analyzing power for excitation of the T=0 state by 200 and 400 MeV protons from the TRIUMF cyclotron with the objective of improving our knowledge of the tensor-exchange part of the nucleon-nucleon interaction. The data at 200 MeV have been superseded by the much higher resolution data from IUCF[5] so only the 400 MeV results are presented here. Experimental techniques are described in detail in a paper with the above title which should be published in Physical Review C in the Fall, 1991.

The cross section and analyzing power for the 0^-;T=0 state are shown in Fig. 1. The optical potential for the calculations were generated by a conventional folding procedure. Inelastic transitions in impulse approximation were obtained from PH[6] and LF[7] interactions and a simple $(1p_{1/2}^{-1}2s_{1/2})$ wave function. Also shown in this figure is a DREX calculation[4] which uses a relativistic framework.

All calculations predict a large positive analyzing power at forward angles while the experimental values are clearly negative. The use of a two-component wave function can alter the magnitude and shape of the cross section somewhat but has little effect on the analyzing power.[5] As the analyzing power arises from interference effects, it may be that the tensor components of the LF and PH interactions[6,7] are incorrect. Similarly, the DREX calculation may suffer from an error in the assumed exchange contribution. There are, however, other effects that should be investigated before using the present results to try to improve the effective interactions.

Isospin mixing between the two 0^- state in ^{16}O at the 5 to 10 % level is known to occur. However, this is insufficient to explain the present results as almost complete mixing is required to produce large negative analyzing power values at forward angles. The 3^- state at 6.130 MeV is strongly excited by intermediate energy protons while the excitation of the 0^- state via the 3^- state competes with the direct excitation.

We have carried out a simplified distorted wave impulse approximation (DWIA) to estimate the effect of a two-step excitation of the 0^- state. The nucleon-nucleon t-matrix is approximated by

$$t_{NN}(q,Q) \approx V^C(q) + V^\sigma(q)\vec{\sigma}_1 \cdot \vec{\sigma}_2. \qquad (1)$$

The $V^C(q)$ and $V^\sigma(q)$ amplitudes are known from NN scattering and were fitted at each energy to a sum of Yukawa forms. Five complex terms were found to give an adequate fit for angles less that 60°. Configuration space potentials were then written in terms of these fitted amplitudes. A $(1p_{1/2}^{-1}2s_{1/2})$ Woods-Saxon wave function was used for the 0^- state. Excitation of the 0^- state directly or via a two-step excitation via an intermediate $(1p_{1/2}^{-1}1d_{5/2})_{3^-}$ state was considered. The cross section for excitation of the 3-- state by 200 MeV protons is shown in Fig. 2 (data from J.J. Kelly); the calculated cross section has been multiplied by a factor of two to account for the known collective nature of the state. This one-step excitation is adequately described in this simple model

A second order DWIA was carried out for both a pure two-step excitation and for a coherent combination of one-step and two-step excitation of the 0^- state by both 200 and 400 MeV protons. The 400 MeV calculations are compared with the present 400 MeV data in Fig. 3. Although the two-step contribution to the cross section is not very significant, the coherent sum of one- and two-step processes has a marked effect on the analyzing power. Both cross section and analyzing power data at 400 MeV are qualitatively described by this calculation. In particular, it is the only calculation to give strongly negative analyzing power at forward angles via a physically plausible mechanism. The situation at 200 MeV is not so clear. Although the calculated analyzing power is smaller in magnitude that that given by more sophisticated calculations, it still does not give a good description of the data.

It is apparent that interference from two-step excitation via the 3^- state masks other contributions to the excitation process at 400 MeV. Thus, there is no possibility of extracting information about the tensor-exchange component of the nucleon-nucleon interaction from the present data. At 200 MeV the two-step process is of less importance and it might be possible to account for its effect (as well as that of isospin mixing) and thereby learn something about the tensor-exchange interaction. However, this would require a more sophisticated treatment of the two-step process.

A paper describing this work has been accepted for publication in Physical Review C. The referee's comment was "This is a nice piece of work that provides an important caveat to a number of ongoing programs in medium-energy nuclear physics."

1. S.S.M. Wong *et al.*, Phys. Lett. **149B** 299 (1984)
2. W.G. Love, M.A. Franey and F. Petrovich, in *Spin Excitations in Nuclei*, edited by F. Petrovich *et al.* (Plenum, New York, 1984),p. 205
3. J. Piekarewicz, Phys. Rev. C **35**, 675 (1987)
4. E. Rost and J.R. Shepard, Phys. Rev. C **35**, 681 (1987)
5. R. Sawafta *et al*, in *Indiana University Cyclotron Facility Scientific and Technical Report, May 1988-April 1989*, edited by E.J. Stephenson, p. 19; to be submitted to Phys. Rev. C

6. H.V. vonGeramb, in *The Interaction Between Medium Energy Nucleons in Nuclei*, 1982, AIP Conf. Proc. No. 97, edited by H.O. Meyer (AIP, New York, 1983), p. 44
7. W.G. Love and M.A. Franey, Phys. Rev. C **24**, 1073 (1981); C **27**, 438 (1983)

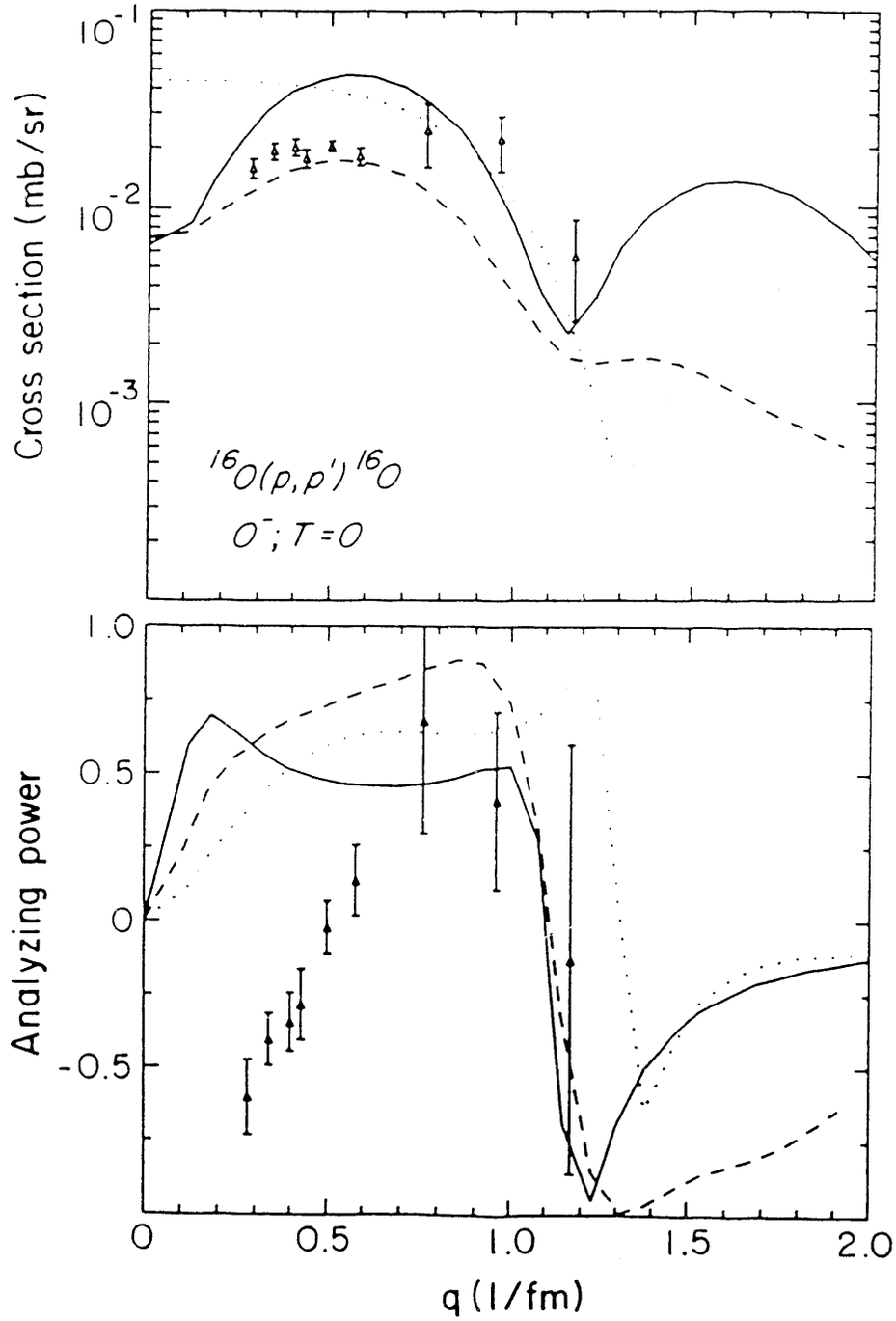

Fig. 1. Cross section and analyzing power for the excitation of the 0^-;T=0 state at 10.957 MeV by 400 MeV protons. The solid lines are from a non-relativistic calculation using the Paris-Hamburg effective interaction. The dotted lines are from a similar calculation using the Love-Franey interaction. The dashed curves are from a relativistic calculation with explicit exchange (DREX).

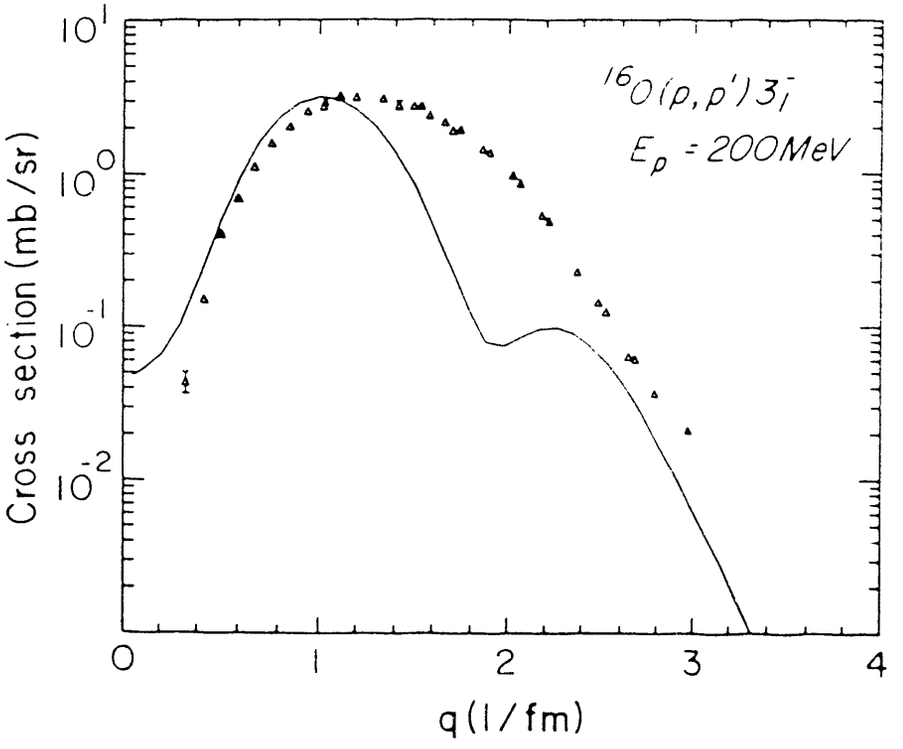

Fig. 2. Experimental and theoretical cross sections and analyzing powers for the excitation of the 3^- state at 6.130 MeV by 180 MeV protons. The data are from J.J. Kelly. The theoretical curve is obtained from a simple first-order impulse approximation and includes a renormalization factor of 2.

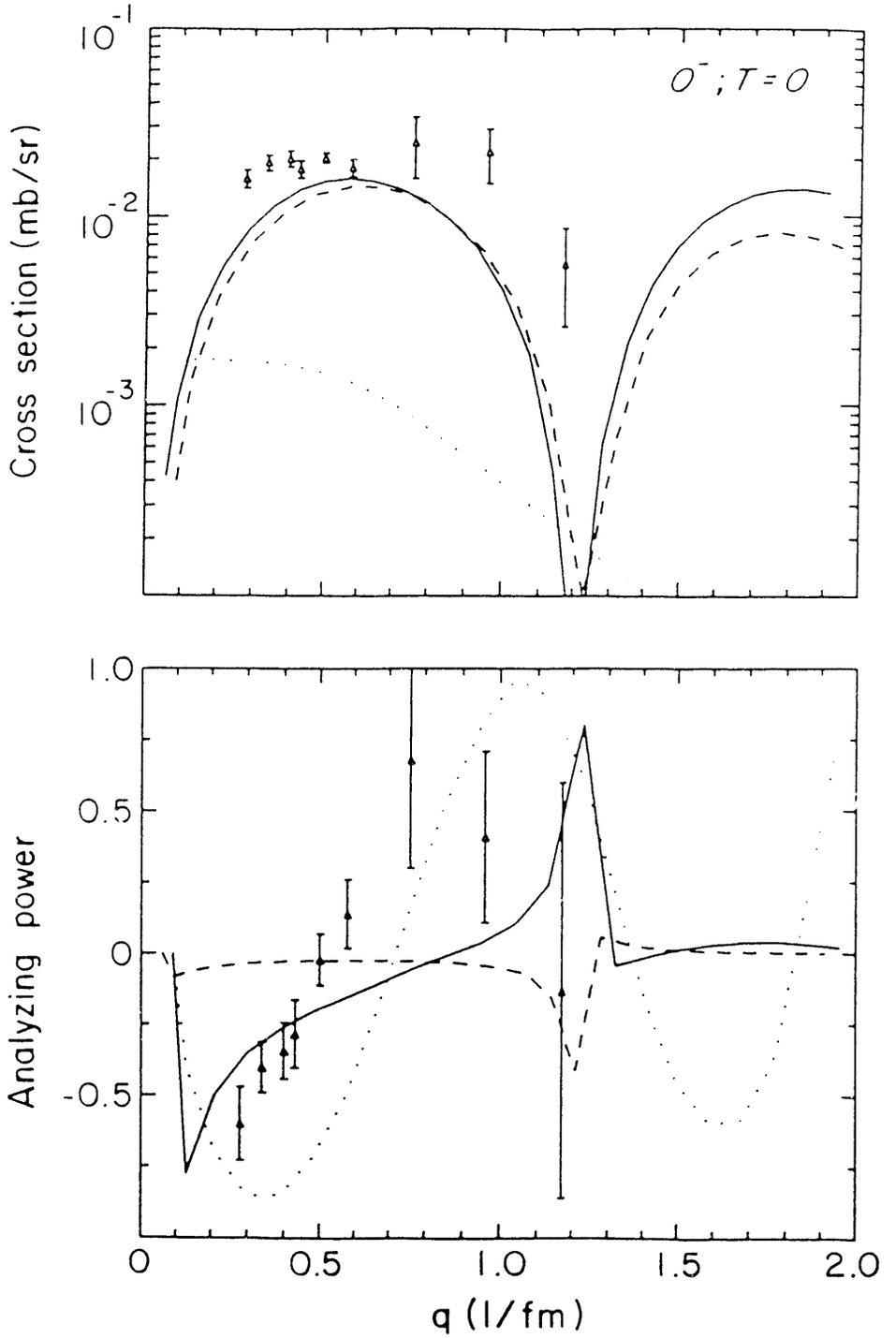

Fig. 3. Experimental and theoretical cross sections and analyzing powers for the excitation of the 10.957 MeV 0^- level of ^{16}O by 400 MeV protons. The dashed curve is obtained from a simple first-order impulse approximation described in the text. The dotted curve is obtained from a second-order DWIA via an intermediate 3^- state. The solid curve is obtained from both one- and two-step processes.

7. **Deformed Chiral Nucleons** C. E. Price and J. R. Shepard

The fundamental field theory of the strong interaction, QCD, has not yet evolved to a form which makes possible quantitative, first-principle calculations of low-energy hadronic properties. Nevertheless, there is general agreement that, when such calculations are done, they will be consistent with the ideas of quark confinement and hidden chiral symmetry. Much effort has been expended to develop phenomenological field theories which are at once calculationally tractable and also to some degree compatible with QCD. A familiar example is that of the Skyrme model[1] which can be interpreted as the large N_c limit of low-energy QCD[2] and whose topological solitons possess both the properties of absolute confinement and hidden chiral symmetry. It is both the strength and weakness of the Skyrme models that they make no explicit reference to quarks. Non-topological soliton (or hybrid) models[3] have been put forward as alternatives which include quark degrees of freedom throughout. These models still possess hidden chiral symmetry but the quarks are not absolutely confined. This latter shortcoming, it may be argued, should not be distressing provided the binding energy of the quarks in hadrons is large on the scale set by our definition of the "low-energy" hadronic properties we seek to describe. In any case, such hybrid models, typically based on elaborations of the Lagrangian of the σ-model,[4] can provide very economical descriptions of, *e.g.*, the N-Δ system. For example, the calculations of Birse and Banerjee[3] and reproduce with reasonable accuracy nucleon properties such as rest mass, magnetic moments, rms radii, g_A and $g_{\pi NN}$ with essentially two free parameters, namely the coupling constant g for the interaction between the quarks and the chiral field (or equivalently, the effective quark mass) and m_σ, the mass of the scalar meson. These and virtually all other hybrid model calculations employ the "hedgehog" ansatz. This amounts to assuming that the pion field has the form $\vec{\pi} = \pi\hat{r}$ and then calculating an intrinsic state in which isospin $\vec{I}$ and angular momentum $\vec{J}$ are coupled to yield a state for which the "grand spin" $\vec{K} = \vec{I} + \vec{J}$ is a good quantum number. Since the matrix elements of the quark spin and isospin operators are readily evaluated for such states, significant calculational simplifications are achieved. More significantly, it has been shown that the hedgehog is a local minimum of energy at least with respect to some restricted variation.[5] However, it is also true that the hedgehog is an unphysical object and physical states with well defined $\vec{I}$ and $\vec{J}$ must be projected from it much as, in the standard treatment of deformed nuclei, states of "good" angular momentum must be projected from a deformed intrinsic state.

With these difficulties in mind, we have developed an alternative to the hedgehog model which utilizes techniques employed in calculations of deformed nuclear ground states[6] in the framework of quantum hadrodynamics (QHD),[7] a relativistic quantum field theory of nuclear structure. We begin with the standard Lagrangian of the nonlinear σ model (see, *e.g.*, Reference 3) including a chiral symmetry breaking term that generates a quark mass (through the non-zero vacuum expectation value of the σ field). Our method diverges from the hedgehog approach in that we assume our three-quark wave functions have spin-isospin structure corresponding to the usual SU(6) wave function for a spin-up proton. Our solutions therefore possess the proper spin and isospin *projections* by construction. Furthermore, if the single quark wave functions were degenerate, our nucleon would have the correct *total* isospin, as well. If we assume

the quarks are in s-states, the equation of motion for the neutral pion field implies $\pi_0 \propto \cos\theta$ where $\theta = \hat{r} \cdot \hat{z}$ is the usual polar angle (charged pion mean fields do not contribute in this model). The pi-quark interaction can then couple, *e.g.*, the lower component of an $s_{1/2}$ quark wave function to the upper component of a $d_{3/2}$ wave function. This means that the neutral pion field can induce deformations in our mean-field solution for the nucleon. We allow for this possibility in our calculations and find single quark wave functions whose energies are split by their interaction with the π_0 field which changes sign upon flip of either spin or isospin. However, this splitting is not large and we have estimated isospin projection by itself to be a 5 to 10% effect at most. If we ignore this small violation of isospin symmetry, we conclude that we have calculated an object intermediate between the hedgehog intrinsic state which is a mixture of various spins *and* isospins and the physical state which has unique values of spin and isospin. Of course we still face the task of projecting physical states of good total angular momentum as is done in standard treatments of deformed nuclei.

	Spherical	Deformed	Hedgehog	Experiment
$(E-m)_1$	-1328 MeV	-950 MeV	-469.5	-
$(E-m)_2$	-413 MeV	-724 MeV	-469.5	-
M_N	1149/693 MeV	1502/1158 MeV	1116 MeV	939/1086 MeV
$\langle r^2\rangle_q^{1/2}$	0.68 fm	0.71 fm	-	-
$\langle r^2\rangle_{ch,p}^{1/2}$	0.66 fm	0.70 fm	-	0.85 fm
μ_p	1.79 nm	2.85 nm	2.87 nm	2.79 nm
μ_n	-1.54 nm	-2.00 nm	-2.29 nm	-1.91 nm
g_A	3.63	1.255	1.86	1.25
$g_{\pi NN}\ m_\pi/2M$	3.47	0.98	1.53	1.00
$\sigma_{\pi N}$	115 MeV	118 MeV	92.5 MeV	59 MeV

Table 1. Experimental and calculated nucleon properties. The spherical and deformed calculations refer to the present work with m_q=1200 MeV and m_σ=600 MeV. The hedgehog calculations are from Reference 3 (see also Reference 8 for corrections to the published results) and assume m_q=500 MeV and m_σ=1200 MeV. The quantity $(E-m)_1$ is the binding energy for the $u_\uparrow$ and $d_\downarrow$ single quark wave functions while $(E-m)_2$ refers to the other pair. RMS radii for the vector quark density and the proton charge density are quoted along with proton and neutron magnetic moments, the axial vector coupling constant and the πNN coupling constant. The σ-nucleus commutator $\sigma_{\pi N}$ is discussed in, *e.g.*, References 3 and 9. Its experimental value is taken from Reference 9. Both the nucleon mass and the average N-Δ mass appear for the experimental value of M_N. Values with and without the center-of-mass correction are displayed for our spherical and deformed calculations.

In Table 1, we compare the results of our calculation of nucleon properties with

those of Birse and Banerjee[3,8] and with experiment. Our (Birse and Banerjee's) calculations use best-fit parameters $m_q = 1200$ (500) MeV and $m_\sigma = 600$ (1200) MeV. We show two sets of our results, one designated as "spherical" which includes only $s_{1/2}$ quark wave functions and another labelled "deformed" which allows up to $g_{7/2}$ admixtures. In the deformed (spherical) calculation, the σ' field has $L = 0$ and 2 ($L = 0$) multipoles while the π_0 field has $L = 1$ and 3 ($L = 1$). We have determined empirically that higher multipoles in either the quark wave functions or the meson fields are of negligible importance. The major difference between the spherical and deformed calculations is due to the presence of the $d_{3/2}$ components in the quark wave functions. The amount of deformation may thus be quantified in terms of the amplitude of the $d_{3/2}$ component of the quark wave functions and is found to be 14% for the deformed calculations presented in Table 1. Another measure of the departure from sphericity is the standard deformation parameter which is $\beta_2 = -0.26$ (for the quark scalar density) in the present case indicating an oblate deformation. As the numbers in the table show, this modest deformation has profound effects on the nucleon properties. Deformation reduces the $u_\uparrow/d_\downarrow$ versus $u_\downarrow/d_\uparrow$ splitting by 690 MeV (to only 224 MeV), increases the total mass by 353 MeV, changes the magnetic moments by about 45% and reduces g_A and $g_{\pi NN}$ by nearly a factor of three putting them in essentially exact agreement with experiment! (Note that g_A and $g_{\pi NN}$ are constrained to be proportional by the Goldberger-Trieman relation, $g_A M = g_{\pi NN} F_\pi$, which is realized at the level of $g_A M/g_{\pi NN} F_\pi = 0.961$ (0.785) for our deformed (spherical) calculation.) Perhaps the most striking difference between our calculations and those for the hedgehog is that our pion field (and hence, its contribution to the nucleon mass) is much smaller than that of the hedgehog. The weakness of our π_0 field is closely connected with the deformation of the quark wave functions. Recall that the π_0 field has a $\cos\theta$ spatial dependence and is therefore strongest at the nucleon "poles" and vanishes at the "equator." Though the interaction of the quarks with this field is attractive for $u_\uparrow$ and $d_\downarrow$ and repulsive otherwise, the total nucleon energy is minimized by minimizing the π_0-quark interaction. In the present model, this is accomplished by an oblate deformation which effectively concentrates the quarks in the "equatorial" region. In turn, this weakens the π_0 source and finally the overall π_0 field strength.

Except for the mass which is subject to sizeable reductions due to center-of-mass corrections, the deformed calculations of the properties of the nucleon are in excellent agreement with experiment. Furthermore, no parameter combination could be found which gave even *remotely* comparable agreement for the spherical calculation. Deformation is evidently a crucial degree of freedom in this model! Again except for the mass, our deformed calculation gives a description of the nucleon which in almost every instance is comparable or superior to that of the hedgehog. The values of g_A and $g_{\pi NN}$ in particular are much better accounted for by the deformed calculation. Only our value for the σ-nucleus commutator,[3,9] $\sigma_{\pi N}$, is in substantial disagreement with experiment[9] and in fact is somewhat worse than the hedgehog result. Regardless of how the two models fare in comparisons with data, perhaps the most interesting result is that they require such different inputs to describe the nucleon. In fact, our calculations do not generate a bound system when we use the Birse and Banerjee best-fit parameters. These differences in values of m_q and m_σ are difficult to understand and provide a strong incentive to understand the formal relation between deformed and hedgehog solutions. This will be the subject of a future publication.

While differences between best-fit parameters for the deformed and the hedgehog solutions are noteworthy in their own right, the specific values we find for m_q and m_σ

have their own interesting implications. We mentioned above that hybrid models such as ours do not give absolute confinement. The energy scale on which the quarks are *effectively* confined is given by the quark binding energy. In the Birse and Banerjee hedgehog, as shown in Table 1, this energy is ~470 MeV. By taking the average of our quark binding energies with weights fixed by the SU(6) wave functions, our quark binding energy is found to be 900 MeV (1125 MeV) for the deformed (spherical) calculation. Thus our quarks are substantially better confined than those of the hedgehog.

As mentioned earlier there are two important limitations of our calculations; 1) lack of angular momentum and isospin projection, and 2) no contributions from charged pions. These two problems may be addressed simultaneously via meson coherent states.[10] A meson coherent state is defined by the relations:

$$\hat{a}\,|z\rangle = z\,|z\rangle \qquad \hat{a}^\dagger = \frac{\partial}{\partial z}\,|z\rangle$$
$$\langle z|\,\hat{a}^\dagger = \langle z|\,z^* \qquad \langle z|\,\hat{a} = \frac{\partial}{\partial z^*}\,\langle z|$$

where $|z\rangle$ is the coherent state characterized by the c-number z and $\hat{a}$ ($\hat{a}^\dagger$) is a meson destruction (creation) operator. For our sigma meson such a state can be written as:

$$|z\rangle = \sum_n \frac{(z\hat{a}^\dagger)^n}{n!}\,|0\rangle = \exp(z\hat{a}^\dagger)\,|0\rangle = \sum_n \frac{z^n}{\sqrt{n!}}\,|n\rangle$$

where $|n\rangle$ is the usual n-meson state. One advantage of a coherent state for the mesons is that it provides a justification of the usual mean-field substitution:

$$\langle z|\,\hat{\sigma}\,|z\rangle = \sigma(\vec{r})$$

where the c-number z is simply related to the mean-field $\sigma(\vec{r})$. Since $|z\rangle$ contains components with all possible numbers of mesons, the expectation value of a single meson operator need not be zero.

For the pion field, which is an isovector, the coherent state is more complicated. Since the nucleon has a definite isospin, it is inappropriate to think of it as involving a state with an arbitrary number of uncorrelated pions. It is, therefore, necessary to form the coherent state for the pion by including the proper coupling to the quarks so that the final nucleon state has the desired quantum numbers. We have approached this problem by writing two pion states, one involving only even numbers of pions and one involving only odd numbers of pions. In each of these states the pions are coupled pairwise to zero total isospin. In other words the even state involves all possible numbers of di-pions (two pions coupled to isospin zero), and the odd state involves all possible numbers of di-pions and one unpaired pion whose quantum numbers determine the quantum numbers of the odd pion state. Then each of these states is coupled to the three quarks to form a nucleon. This treatment of the mesons means that our proton is really a combination of a 'bare' proton (three quarks only) plus a 'bare' neutron coupled to a π^+ plus higher order components involving 'bare' deltas, other nucleon resonances and higher numbers of pions.

Given this starting point, it is then a simple matter to write down a set of coupled mean-field equations for the quark wave-functions and the sigma and pi fields, which automatically include the proper angular momentum and isospin quantum numbers. Then, standard techniques for solving mean-filed equations[6] lead to a self-consistent nucleon solution that incorporates projection before variation. Numerical calculations for this approach are in progress.

1. T.H.R. Skyrme, Proc. R. Soc. London **A260** 127 (1961); Nuclear Physics **31** 556 (1962); J. Math. Phys. **12** 1735 (1971)
2. E. Witten, Nuclear Physics **B223** 422 (1983); Nuclear Physics **B223** 433 (1983); G. Holzwarth and B. Schwesinger, Reports on Progress in Physics **49** 825 (1986)
3. M.C. Birse and M.K. Bannerjee, Physics Letters **136B** 284 (1984); Physical Review **D31** 118 (1985)
4. M. Gell-Mann and M. Levy, Nuovo Cimento **16** 705 (1960)
5. K. Goeke, J.N. Urbano, M. Fiolhais and M. Harvey, Physics Letters **164B** 249 (1985)
6. R.J. Furnstahl and C.E. Price, Physical Review **C40** 1398 (1989)
7. B.D. Serot and J.D. Walecka, in *Advances in Nuclear Physics, Vol. 16, J.W. Negele and E. Vogt, eds.*, Plenum, N.Y. (1986)
8. W. Bronioski and M. K. Banerjee, Physics Letters **158B** 335 (1985)
9. J. Gasser, H. Leutwyler, M.P. Locher and M.E. Sainio, Physics Letters **213B** 85 (1988)
10. P. Ring and P. Schuck, 'The Nuclear Many-Body Problem', Springer-Verlag, New York (1980)

8. Alternate Basis For Exact Vacuum Calculations in 3-Spatial Dimensions J.R. Shepard, J. Garten and C. E. Price

As reported in Section 2, we have successfully developed an efficient numerical procedure for exactly renormalizing one-loop vacuum contributions to the ground states of finite nuclei in a version of QHD for one spatial dimension. As is well-known, extension of one-dimensional techniques to three spatial dimensions is highly non-trivial. In the present case, for example, the crucial "completeness" relation exploited in one dimension which emerges because the free basis consists of sines and cosines cannot be readily duplicated in three dimensions using the usual free basis constructed from spherical Bessel functions.

In a search for a more convenient basis in three dimensions we are examining solutions to the free wave equation in *four* Euclidean dimensions. The fundamental idea is most simply explained by considering how the usual 3-D basis may be used to deal with 2-D problems. Specifically if we begin with a 3-D spherical coordinate system, we may fix the 3-D radius and so define a spherical surface in 3-D:

$$(r, \theta, \varphi) \rightarrow (R, \theta, \varphi).$$

Restricting our attention to a region near the "north pole" ($\theta \sim 0$) we may establish a correspondence between the remaining 3-D coordinates and the usual polar coordinates in 2-D:

$$(\rho_2, \varphi_2) \leftrightarrow (R\theta_3, \varphi_3)$$

where R is the radius of the 3-D sphere. In the limit $\rho_2/R \rightarrow 0$, this correspondence becomes exact. In very specific terms, the correspondence includes the following mathematical relation.

$$P_\ell^m(\cos\frac{\rho}{R}) \leftrightarrow J_m(\sqrt{\ell(\ell+1)}\rho/R)$$

which is *very* well satisfied for

$$a)\ \ \ell \geq 3 \ \text{ and } \ b)\ \ \rho/R \leq 0.5 \quad .$$

In 4-D, one may choose a hypersphere of radius R to correspond to the usual 3-D space. Here the correspondence becomes

$$U_n^\ell(\cos\ r/R) \leftrightarrow j_l(\sqrt{n(n+2)}\rho/R)$$

where $U_n^\ell(x)$ is an associated Chebyshev polynomial of the second kind. For example,

$$U_n^{\ell=0}(\cos\theta) \propto \frac{\sin(n+1)\theta}{\sin\theta} \quad .$$

The extent to which the basis constructed from the U_n^ℓ's can be exploited for treating one-loop vacuum contributions to finite systems in 3-D is presently being investigated.

9. Second Order Processes in the $(e, e'd)$ Reaction

P.D. Kunz and H.P. Blok (NIKHEF)

The knockout of protons in the $(e, e'p)$ reaction has given useful information concerning single particle density functions in nuclei. This reaction is easier to interpret than the $(p, 2p)$ or $(d, {}^3He)$ reactions since it proceeds via the well understood and relatively weak coulomb interaction. In light nuclei the distortion of the electron waves can be neglected so that the transition amplitude factorizes rather accurately into a coulomb amplitude and a factor which depends upon a matrix element involving the bound and free proton states. No other strongly interacting particles are involved. Studies of these reactions have encountered puzzling and interesting features such as the observed enhancement of the transverse to longitudinal strength and the low extracted occupation probabilities for the bound protons.

The extension of these experiments to the $(e, e'd)$ reaction allows the additional study of correlations between nucleons. Information about the two-nucleon density function is sparse in contrast to the $(e, e'p)$ reaction. The extraction of this function via two-nucleon pickup reactions, *e.g.* the $(p, {}^3He)$ and (p, t) reactions has been plagued by uncertainties in the basic reaction mechanisms. For example, the controversy over the roles of the direct versus sequential transfer modes has not yet been resolved satisfactorily. In addition any model used to compute the cross sections for these cases faces the problem of dealing with at least three strongly interacting active particles outside a nuclear core. Thus, any reduction of the many body problem is welcome and in the case of the $(e, e'd)$ reaction the factorization of the transition amplitude give a more tractable problem to solve than in the case of the usual pick-up reactions. Hopefully, one can obtain unambiguous information about the two-nucleon density function. Since full coincident measurements of the two outgoing nucleons are not feasible at this time, we consider only those aspects of the correlations that can be studied with one outgoing particle.

One important important issue to be addressed for this reaction is the basic understanding of the reaction mechanism. In particular, how much do the higher order processes affect the extraction of useful nuclear structure information as they do in reactions such as the (p,t) reactions.[1] Perhaps higher order processes in the $(e, e'd)$ reaction are also important. One higher order process which can contribute to the reaction involves the continuum channels in the knockout of the deuteron. The free neutron and proton then recombine in the field of the nucleus to reform as the ground state of the deuteron. Our goal is to assess the role and importance of this mechanism which must be understood before useful information can be derived from the reaction.

Theory

Our model treats the $A(e, e'd)B$ reaction in terms of an electron, a proton and a neutron outside of an inert core B with the nuclear degrees of freedom appearing only in the form of an imaginary part of the nucleon-nucleus potential. The Hamiltonian for this system is given by

$$H = H_B(\xi_i) + K_e + K_p + K_n + v_{pn} + v_{ep} + V_e + V_p + V_n, \qquad (1)$$

where the K's are the kinetic energy operators for the three particles, v_{pn} is the internucleon interaction and $V_p(\mathbf{r}_p) + V_n(\mathbf{r}_n)$ is the sum of the optical potentials of the

proton and neutron with the core B evaluated at half the deuteron kinetic energy. The interaction $v_{ep} + V_e$ is the coulomb interaction of the electron with the target nucleus and $H_B(\xi_i)$ is the hamiltonian of the core. The $V_p + V_n$ may contain an imaginary part to take into account absorption from channels that are neglected in our model. In the limit of a weak electromagnetic interaction and treating the electron as a plane wave, the transition amplitude for the deuteron knockout is

$$T_{fi} = \left\langle \Phi^-_{f,A}(\mathbf{r}_\mathrm{p}, \mathbf{r}_\mathrm{n}, \xi_i) e^{i\mathbf{k}_\mathrm{f}\cdot\mathbf{r}_\mathrm{e}} \mid v_{ep} \mid \Phi_{i,A}(\mathbf{r}_\mathrm{p}, \mathbf{r}_\mathrm{n}, \xi_i) e^{i\mathbf{k}_\mathrm{i}\cdot\mathbf{r}_\mathrm{e}} \right\rangle. \tag{2}$$

In the above amplitude the electron coordinates are taken to be relative to the initial target A, while the nucleon coordinate are taken relative to the core B. The functions $\Phi_{i,A}(\mathbf{r}_\mathrm{p}, \mathbf{r}_\mathrm{n}, \xi_i)$ and $\Phi^-_{f,A}(\mathbf{r}_\mathrm{p}, \mathbf{r}_\mathrm{n}, \xi_i)$ satisfy the Hamiltonian for the three body system

$$H_d = H_B(\xi_i) + K_p + K_n + v_{pn} + V_p + V_n. \tag{3}$$

The solution for the initial state $\Phi_{i,A}(\mathbf{r}_\mathrm{p}, \mathbf{r}_\mathrm{n}, \xi_i)$ describes a bound state of the proton and neutron and may be given by a shell model solution. The solution for the final state $\Phi^-_{f,A}(\mathbf{r}_\mathrm{p}, \mathbf{r}_\mathrm{n}, \xi_i)$ describes the outgoing deuteron of energy E_{cm}. The transition amplitude now can be expressed as

$$T_{fi} = v_{ep}(q,\omega) \left\langle \Phi^-_{f,A}(\mathbf{r}_\mathrm{p}, \mathbf{r}_\mathrm{n}, \xi_i) \mid e^{i\mathrm{q}\cdot\mathrm{r}/2} \mid \Phi_{i,A}(\mathbf{r}_\mathrm{p}, \mathbf{r}_\mathrm{n}, \xi_i) e^{i(B/A)\mathrm{q}\cdot\mathrm{R}} \right\rangle. \tag{4}$$

where $\mathbf{q} = \mathbf{k}_\mathrm{i} - \mathbf{k}_\mathrm{f}$ is the momentum transfer of the electron and $v_{ep}(q,\omega)$ is the coulomb amplitude for a momentum transfer q and energy transfer ω.

In earlier calculations[2] the potential $V_p(\mathbf{r}_\mathrm{p}) + V_n(\mathbf{r}_\mathrm{p})$ in the final state is approximated by an optical potential $U_d(\mathbf{R})$ which depends only on the deuteron center of mass coordinates. Thus, the solution can be factored into the form,

$$\Phi^-_{f,A}(\mathbf{r}_\mathrm{p}, \mathbf{r}_\mathrm{n}, \xi_i) \approx \chi^-_0(\mathbf{R}) \phi_0(\mathbf{r}) \phi_B(\xi_i) \tag{5}$$

where $\phi_0(\mathbf{r})$ is the deuteron ground state for the internal motion, $\chi^-_0(\mathbf{R})$ is a distorted wave for the center of mass motion and $\phi_B(\xi_i)$ is the core state. The resulting amplitude is the basis for the Distorted Wave Impulse Approximation (DWIA),

$$T_{f,i} = v_{ep}(q,\omega) \left\langle \chi^-_0(\mathbf{R}) \mid \left\langle \phi_0(\mathbf{r}) \mid e^{i\mathrm{q}\cdot\mathrm{r}/2} \mid u(\mathbf{r}_\mathrm{p}, \mathbf{r}_\mathrm{n}) \right\rangle \mid e^{i(B/A)\mathrm{q}\cdot\mathrm{R}} \right\rangle, \tag{6}$$

where the overlap between the initial and final nuclear states is,

$$u(\mathbf{r}_\mathrm{p}, \mathbf{r}_\mathrm{n}) = \left\langle \phi_B(\xi_i) \mid \Phi_{i,A}(\mathbf{r}_\mathrm{p}, \mathbf{r}_\mathrm{n}, \xi_i) \right\rangle. \tag{7}$$

However, in order to take the deuteron breakup states into account the Hamiltonian given by Eq(3) is solved by expanding the solution into eigenstates of the deuteron

internal motion,

$$\Phi^{-}_{f,A}(\mathbf{r}_p, \mathbf{r}_n, \xi_i) = \sum_n \chi_n(\mathbf{R})\phi_n(\mathbf{r}) \tag{8}$$

where $\chi_0(\mathbf{R})$ for the deuteron ground state has boundary conditions of an incoming plane wave plus an ingoing scattered wave and the $\chi_n(\mathbf{R})$ for $n > 0$ have boundary conditions of ingoing wave only. The $\phi_n(\mathbf{r})$ in this work are restricted to be only relative s-wave states and satisfy a boundary condition $\phi_n(r_{max}) = 0$.

The solution of the Schrödinger equation then reduces to an infinite set of coupled equations of the form

$$(E_n - K_R - V_{nn})\chi_n(\mathbf{R}) = \sum_{n \neq n'} V_{nn'}\chi_{n'}(\mathbf{R}) \tag{9}$$

where the coupling potentials are

$$V_{nn'} = \left\langle \phi_n(\mathbf{r}) \,|\, V_p(\mathbf{R} + \mathbf{r}/2) + V_n(\mathbf{R} - \mathbf{r}/2) \,|\, \phi_{n'}(\mathbf{r}) \right\rangle \tag{10}$$

and the channel energy is

$$E_n = E - \epsilon_n. \tag{11}$$

This set of equations is truncated to give a finite set of coupled equations which can be solved by usual methods, *e.g.* by the computer code CHUCK3. The transition amplitude Eq(4) may then be calculated in a straightforward manner.

The radius r_{max} is chosen to give seven to nine states for the deuteron center of mass energy between zero and the maximum energy. For a total energy of about 50 MeV the value of r_{max} was taken to be about 30 fm. The results are insensitive to the value of r_{max} and the center of mass energies near zero are found to contribute insignificantly to the results.

Results

Three type of calculations are performed. The first is the extreme cluster model restricted to the ground state elastic channel for the final deuteron, the second employs a microscopic model to generate the bound states (elastic channel only), while the third uses the full coupled channels method for the deuteron final state. The first calculation with the cluster model generates a bound state wave function for the center of mass of the deuteron in a Woods-Saxon potential with parameters $r_0 = 1.10$ fm and $a_0 = 0.65$ fm. The potential depth is adjusted to give the separation energy of the cluster. A non-locality parameter of 0.62 fm is used. The well radius is chosen to give a close fit to the form factor from the microscopic model and assumes that the deuteron internal motion is the same in the bound state as for the free state. We have used the deuteron optical model parameters of Hintenberger *et al.*[3] The results for the reduced cross section which has the electron-deuteron cross section divided out are shown in Fig. 1. The E_{cm} of the deuteron is 52 MeV and the results are plotted as the dashed line for the 1+ state in ^{10}B versus the missing momentum p_m the momentum of the deuteron relative to the final nucleus. In these calculations the momentum transfer of the electron ranges from 120 MeV/c to 480 MeV/c.

In the microscopic model the form factor is generated from single particle bound states of the neutron and proton. These wave functions were calculated in a Woods-Saxon potential with parameters $r_0 = 1.25$ fm, diffuseness parameter $a_0 = 0.65$ fm and a Thomas spin orbit factor of 25. A non-locality factor of 0.85 fm is used. The potential strength is adjusted to give the average separation energies of the nucleons. The contribution of the various $p_{3/2}$-$p_{1/2}$ combinations of the correlated wave function were taken from the coefficients of fractional parentage of Cohen and Kurath[4] times $\sqrt{28}$ for the number of deuteron pairs. The overlaps of the two single particle wave functions were taken with an internal deuteron wave function of Hulthén form with binding and short-range parameters, 4.318 fm and 0.667 fm, respectively. The results for the reduced cross section shown in Fig. 1 as the dot-dash line.

The third set of calculations for the continuum state coupled channels case uses the same form factor construction as for the microscopic case. The optical potentials for the nucleons are taken from the best fit parameters of Becchetti and Greenlees[5] and the separable potential of Yamaguchi[6] was used for v_{pn}. The results are shown in Fig. 1 as the solid line.

While the cluster and elastic microscopic models follow the trend of the data, their magnitudes exceed it by factors of 2-3 or more. The preliminary results from the coupled channels method shows large changes from the elastic channel calculation, matching the data for small values of the missing mass p_m but overpredicting the data at larger values. Clearly, these results are preliminary and several aspects need closer scrutiny, for example, the need for a more realistic model for the deuteron which includes repulsive core effects and the D states. The D state is known to be important in describing elastic scattering in this model[7].

1. B. Elbek and P.O. Tjom, Adv. Nucl. Phys., **3** 259 (1969); M. Igarashi and K.I. Kubo, Phys. Rev. **C25** 2144 (1987)
2. R. Ent, thesis, Vrije Universiteit Amsterdam (1989)
3. F. Hintenberger, G. Mairle, U. Schmidt-Rohr, G.J. Wagner and P. Turek, Nucl. Phys. **A111** 265 (1968)
4. S. Cohen and D. Kurath, **A141** 145 (1970)
5. F.D. Becchetti and G.W. Greenlees, Phys. Rev. **182** 119 (1969)
6. Y. Yamaguchi, Phys. Rev. **95** 1628 (1954)
7. M. Kamimura *et al.*, Prog. Theor. Phys. Suppl. **89** 1 (1986)

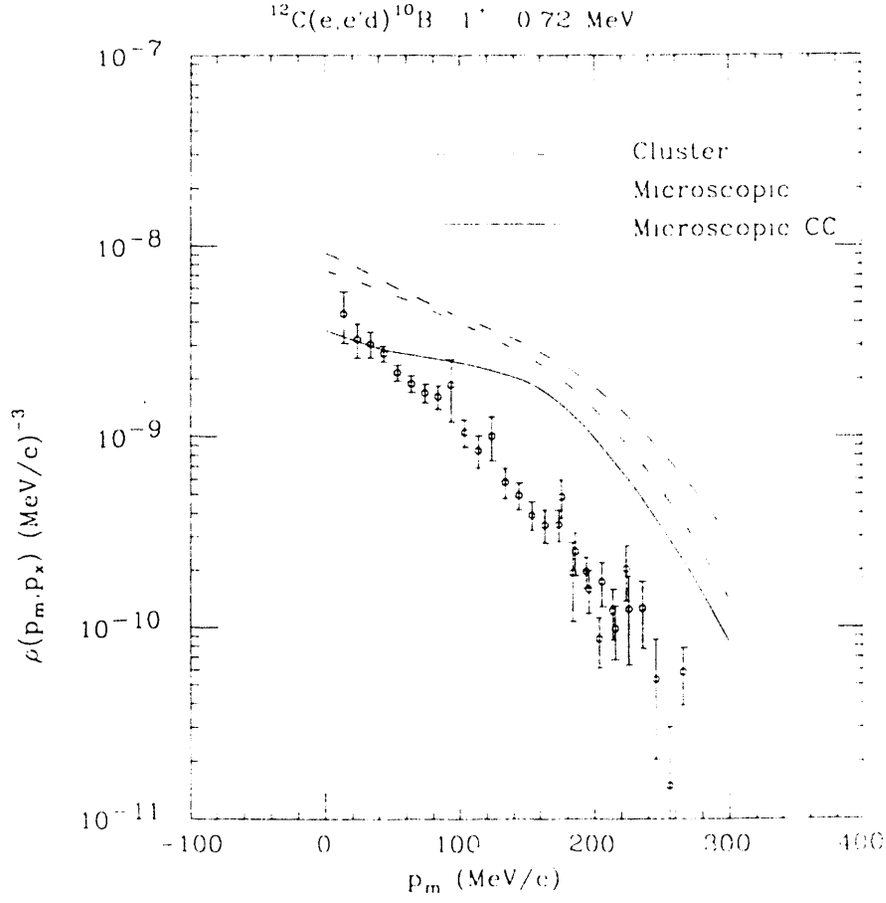

Fig. 1. Measured reduced cross section[2] for the $^{12}C(e,e'd)^{10}B_{0.72MeV}$ reaction compared to the results of the DWIA and coupled channels models.

10. Scalar and Vector contributions to $\bar{p}p \to \bar{\Lambda}\Lambda$ and $\bar{p}p \to \Lambda\Sigma^0 + c.c.$ P.D. Kunz and University of Washington Collaboration (M.A. Alberg, E.M. Henley and L. Wilets)

The reactions $\bar{p}p \to \bar{\Lambda}\Lambda$ and $\bar{p}p \to \bar{\Lambda}\Sigma^0$ can be described in complementary models: meson exchange[1-5] or quark annihilation.[3,6-10] Both approaches provide reasonable fits to the data[11] as long as the effects of initial and final state interactions are included. Because meson exchange occurs at short distances for which quark effects should be important, we present here a calculation based on constituent quark dynamics. We describe our reaction mechanism, the initial and final state interactions, and a comparison of our results with the experimental data.

We have proposed a reaction mechanism which includes both scalar and vector contributions to the annihilation and subsequent creation of quark-antiquark pairs. The simplest graphs for these terms are shown in Fig. 1. The $^3P_0$ term represents the confining scalar force and the $^3S_1$ term describes a vector quantum exchange (e.g. of one or more gluons).

In our model, the operator for vector exchange is

$$I_v = g_v \overleftarrow{\sigma_3'} \cdot \overrightarrow{\sigma_3}$$

and that for scalar exchange is

$$I_s = g_s \overleftarrow{\sigma_3'} \cdot \left(\frac{\overleftarrow{\nabla}_{3'} - \overleftarrow{\nabla}_{6'}}{2m_s} \right) \overrightarrow{\sigma}_3 \cdot \left(\frac{\overrightarrow{\nabla}_3 - \overrightarrow{\nabla}_6}{2m} \right) ,$$

where m_s and m are the strange and up quark masses respectively. Our matrix element for the reaction is

$$\mathcal{M}_{\bar{p}p \to \bar{\Lambda}\Lambda} \sim \langle \chi_{\bar{\Lambda}\Lambda}(1'2'3';4'5'6')\phi(1'2'3')\phi(4'5'6')|(I_v + I_s) \times |\phi(123)\phi(456)\chi_{\bar{N}N}(123;456)\rangle ,$$

in which $\chi_{\bar{\Lambda}\Lambda}$ and $\chi_{\bar{N}N}$ are distorted waves in the relative coordinate between the initial and final particles, respectively, and ϕ is a harmonic oscillator wavefunction of the internal motion of the quarks.

We use the same distorting potentials for $\bar{N}N$ as Kohno and Weise.[3] For $\bar{N}N$ the real part of the potential is determined by a G-parity transformation of the long-range part of a realistic one-boson exchange potential, with a smooth extrapolation to the origin. The imaginary part, which represents annihilation, is of Wood-Saxon form with a radius R = 0.55 fm and diffuseness parameter a = 0.2 fm. The strength of this potential is adjusted to produce good fits to $\bar{p}p$ elastic scattering data. For the real part of the $\bar{\Lambda}\Lambda$ interaction Kohno and Weise use the isoscalar boson exchanges of the real part of the $\bar{N}N$ potential. The annihilation term is taken to be of the same form

as that for the $\bar{N}N$, but with a strength of the imaginary term adjusted to fit total $\bar{p}p \rightarrow \bar{\Lambda}\Lambda$ cross section data. The quark wave function is parameterized in the form of a gaussian

$$\phi \sim \prod_{i<j} exp(-(r_{ij}/r_0)^2).$$

Our results for the differential cross sections are shown in Fig. 2 and the results for the polarizations are shown in Fig. 3. The figures are plotted for the parameter sets shown in Table I. The strengths of the potentials in the table are the scaling factors for the Kohno-Weise potentials needed to obtain the fits. We found unique solutions for the $\bar{p}p \rightarrow \bar{\Lambda}\Lambda$ momenta of 1.546 GeV/c and 1.695 GeV/c, for which the most data (60 and 100 points, respectively), including spin correlation coefficients, were available. At 1.508 GeV/c, and at 1.695 GeV/c for the $\bar{\Lambda}\Sigma^0$ reaction, for which only 25 and 13 data points respectively, were available, two solutions were found with nearly indistinguishable cross sections and polarizations. In all cases the best fits included non-zero contributions from both scalar and vector terms, and strengths of terms in the hyperon-antihyperon potential that differed from those predicted by SU3.

Table I Parameters of best fits to experimental data

Momentum (GeV/c)	g_v	g_s	r_0	W	V	V_T	V_{LS}	χ^2/df
1.508	3.3	0.75	0.68	1.7	-0.43	0.84	-0.45	1.1
	3.1	-1.9	0.72	3.8	-0.44	-4.2	3.2	1.1
1.546	5.6	4.3	0.60	2.5	0.29	-0.26	0.47	2.2
1.695	2.4	1.8	0.66	1.5	-0.01	0.62	0.79	2.7
1.695($\Sigma\Lambda$)	5.1	2.7	0.66	1.5	-0.15	-1.4	0.03	0.6
	6.5	-1.3	0.60	1.3	-0.76	-3.3	1.5	0.6

The main feature of our searches finds the oscillator parameter for the quark bag to be in the range 0.6-0.7 fm compared to the value of 0.64 fm required to describe the constituent quark radius in the nucleons and lambdas. Except for the second solutions in the 1.508 GeV/c $\bar{p}p$ and 1.695 GeV/c $\bar{\Lambda}\Sigma$ cases the results show a destructive interference between the vector and scalar contributions. In addition the strength of the imaginary part of the potential must be increased over that used by Kohno and Weise. One further feature is that the real part of the central potential V is in general much smaller and in most cases of opposite sign to that predicted by the SU3 extension of the $\bar{p}p$ interaction. The dependence of the fits to the tensor and spin orbit potentials is rather weak so that no definite conclusion on these forms can be made. However, the momentum dependence of the parameters in the fits is not monotonic, although there are a number of local minima in the χ^2 space which give nearly as good fits. This

occurs from a correlation between some of the parameters particularly the strengths g_v and g_s. We will make further studies to search for a set of parameter that are more consistent among the various data sets. This further study will include a global search on all data sets simultaneously.

We have shown that a quark model which includes both scalar and vector contributions can provide good fits to experimental data for the $\bar{p}p \to \bar{\Lambda}\Lambda$ and $\bar{p}p \to \bar{\Lambda}\Sigma^0 + c.c.$ reactions. The sensitivity of the results to the parameters of the hyperon-antihyperon potentials may provide information about the hyperon-antihyperon interaction

1. F. Tabakin and R.A. Eisenstein, Phys. Rev. **C31** 1857 (1985)
2. J.A. Niskanen, Helsinki preprint HU-TFT-85-28
3. M. Kohno and W. Weise, Phys. Lett. **B179** 15 (1986); Phys. Lett. B206 584 (1988); Nucl. Phys. **A479** 433c (1988)
4. R.G.E. Timmermans, T.A. Rijken and J.J. deSwart, Nucl. Phys. **A479** 383c (1988)
5. P. LaFrance, B. Loiseau, and R. Vinh Mau, Phys. Lett. **B214** 317 (1988)
6. M.A. Alberg, E.M. Henley, and L. Wilets, Z. Phys. **A331** 207 (1988)
7. C.B. Dover and P.M. Fishbane, Nucl. Phys. **B244** 349 (1984)
8. G. Brix, H. Genz and S. Tatur, Phys. Rev. **D39** 20545 (1989)
9. P. Kroll, B. Quadder and W. Schweiger, Nucl. Phys. **B316** 373 (1989)
10. S. Furui and A. Faessler, Nucl. Phys. **A468** 669 (1987)
11. P.D. Barnes *et al.*, Phys. Lett. **B189** 249 (1987); B229 432 (1989); **B246** 273 (1990); W. Dutty, Dissertation, University of Freiburg (1988); G. Sehl, Dissertation, University of Bonn, Jül-Spez-535 (1989)

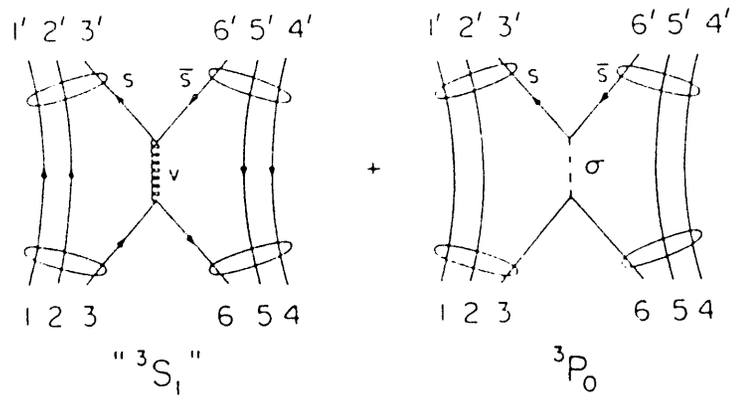

Fig. 1. Lowest order diagrams for $\bar{p}p \to \bar{\Lambda}\Lambda$

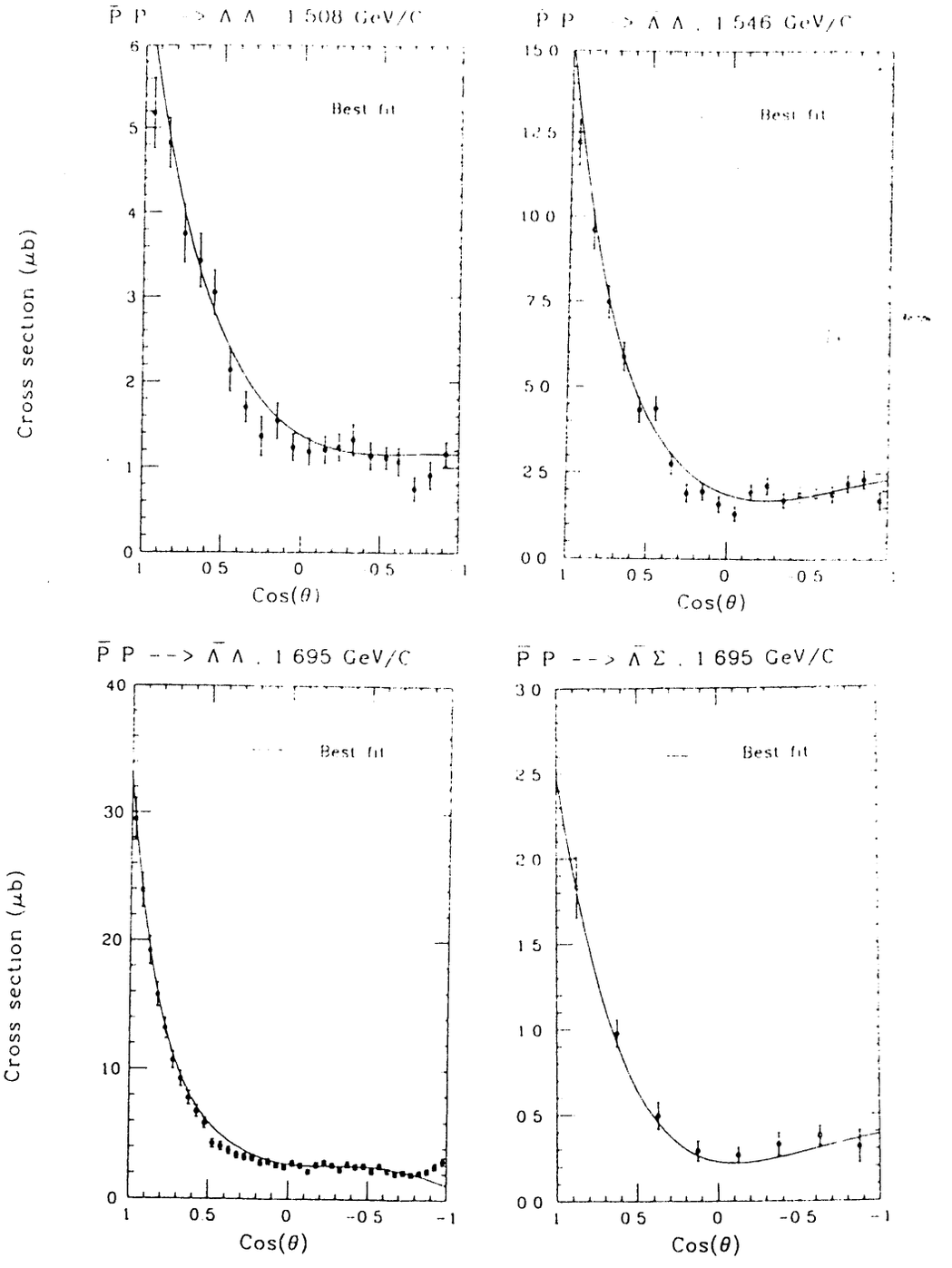

Fig. 2. Comparison of calculations with parameters of Table I with experimental data for the cross section.[11]

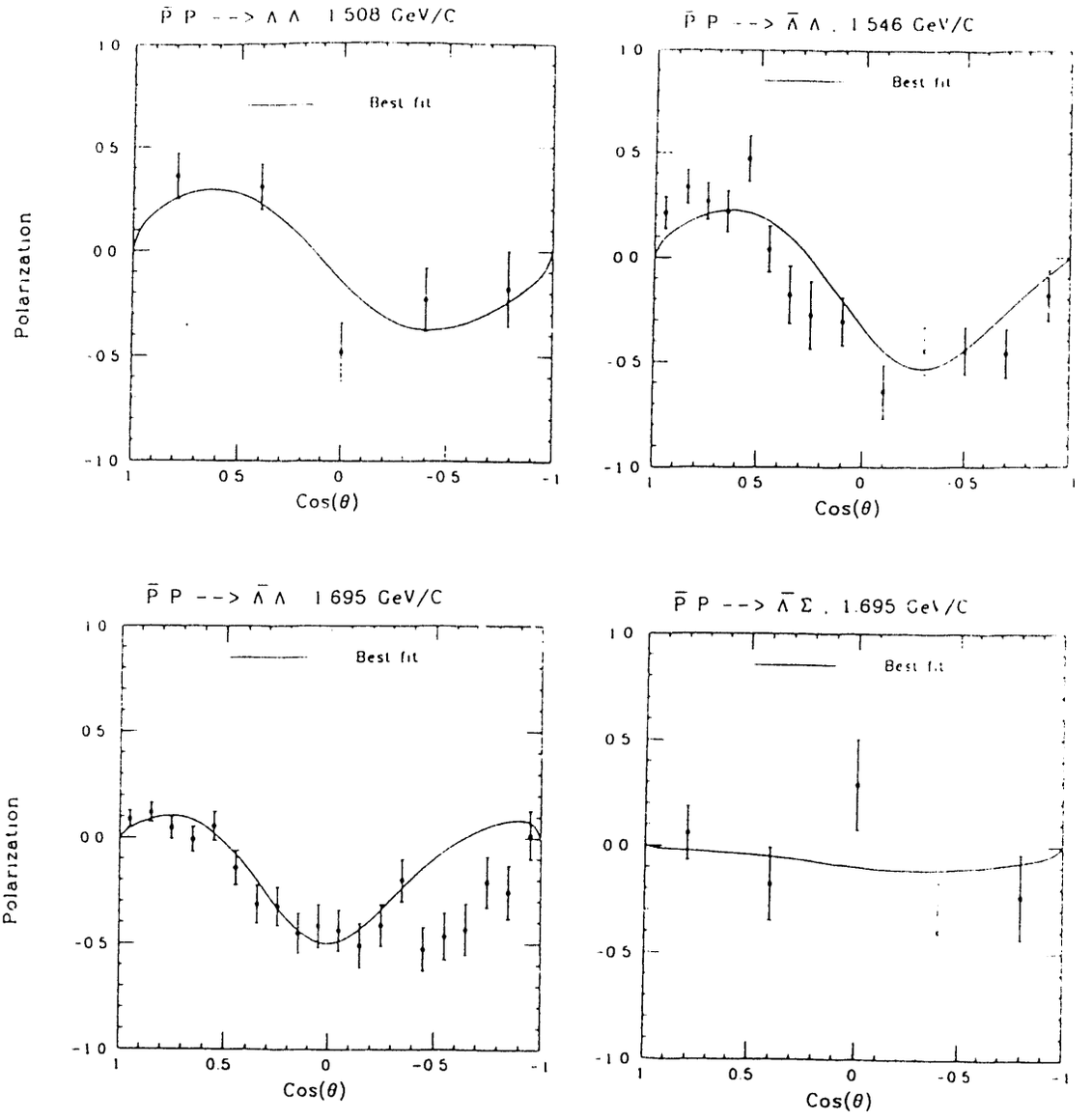

Fig. 3. Comparison of calculations with parameters of Table I with experimental data for the polarization.[11]

11. Radiative Capture of Protons by Light Nuclei at Low Energies

P.D. Kunz (with F.E. Cecil, D. Ferg, H. Liu and J.A. McNeil, Colorado School of Mines.)

As a part of a continuing program of measurements of radiative capture reactions of light ions by low-Z nuclei at low energies, we report work on the radiative capture of protons by ^{6}Li, ^{7}Li, ^{9}Be and ^{11}B at the Colorado School of Mines. The present data and their theoretical analysis will provide a base for the diagnostics of the advanced fuel fusion reactors and in addition should prove applicable to current models of primordial astrophysics nucleosynthesis. There has been, with one exception, no reported measurements of the cross sections for the radiative capture of protons on these targets below about 200 keV. The single exception consists of the well studied resonance reaction, ^{11}B(p,γ)^{12}C, at a proton bombarding energy of 163 keV.[1]

The results of our measurements may be compared to the direct-capture calculations which are closely patterned after those of Rolfs and Tombrello.[2,3] In our calculations, we assumed an s-wave electric dipole capture in the long wave limit. These approximations are well justified at the low energies bombarding energies at which the measurements were taken. The code DWUCK4 was modified to handle the (p,γ) calculation similar to a stripping reaction with a massless outgoing particle of spin 1 to represent the gamma ray. The relevant formula for the cross section is

$$\sigma(E_1) = \frac{16\pi\alpha}{9v_{cm}} \frac{E_\gamma^3 d^2 \mu^2}{\hbar^3 c^2 k_{cm}^2} \frac{(2J_f+1)}{(2J_i+1)} |(j_p \tfrac{1}{2} \tfrac{1}{2} - \tfrac{1}{2}|1\,0)|^2 R(E1)^2. \quad (1)$$

where $d = (Z_p/M_p - Z_T/M_T)$, μ is the reduced mass in atomic mass units and the dipole radial matrix element is defined by

$$R(E1) = \int_0^\infty dr u_f(r) r u_i(r) \quad (3)$$

and $u_i(r)$ is the initial bound and $u_f(r)$ is the final reduced radial wave function with angular momentum 0 and 1 respectively.

The resulting calculated cross sections for the capture of protons to the ground states of ^{7}Be, ^{8}Be, ^{10}B and ^{12}C are shown in Fig. 1. In these calculations we assume unit spectroscopic factors. The measured values of the cross sections are shown as the solid lines. Aside from two discrepancies, our calculations are in good agreement with the measurements. In the case of the $^{11}B(p,\gamma)^{12}C$ reaction our calculation assumes only capture from the continuum s-state and the effect of the 2^+ 163 keV resonance is not included. In the case of the ^{6}Li(p,γ)^{7}Be reaction the calculated cross sections are high by a factor of about five. In this reaction the effect[5] of the initial state interactions in the I = 1/2 channel causes a large cancellation in the matrix element and reduces this cross section by a large factor. In the I = 3/2 channel the cancellation is less severe but again the contribution to the cross section is small since the spectroscopic factor in

this channel is small. Even in the realistic calculation of ref. 4, the cross sections must be renormalized by a factor of two to agree with the data. One possible explanation of the discrepancy in the ^{6}Li(p,γ)^{7}Be reaction is the strong coupling to the break-up states, which may influence the destructive interference in the matrix elements.

In conclusion the main energy dependences of the (p,γ) cross sections are predicted rather well by our crude model but more detailed models need to be developed for each case in order to attain better agreement with the overall magnitudes of the cross sections.

1. F. Ajzenberg-Selove, Nucl. Phys. **A433** 1 (1985)
2. C. Rolfs, Nucl. Phys. **A217** 29 (1973)
3. T. Tombrello and P. Parker, Phys. Rev. **131** 2582 (1963)
5. F.C. Barker, Austr. J. Phys. **33** 159 (1980)

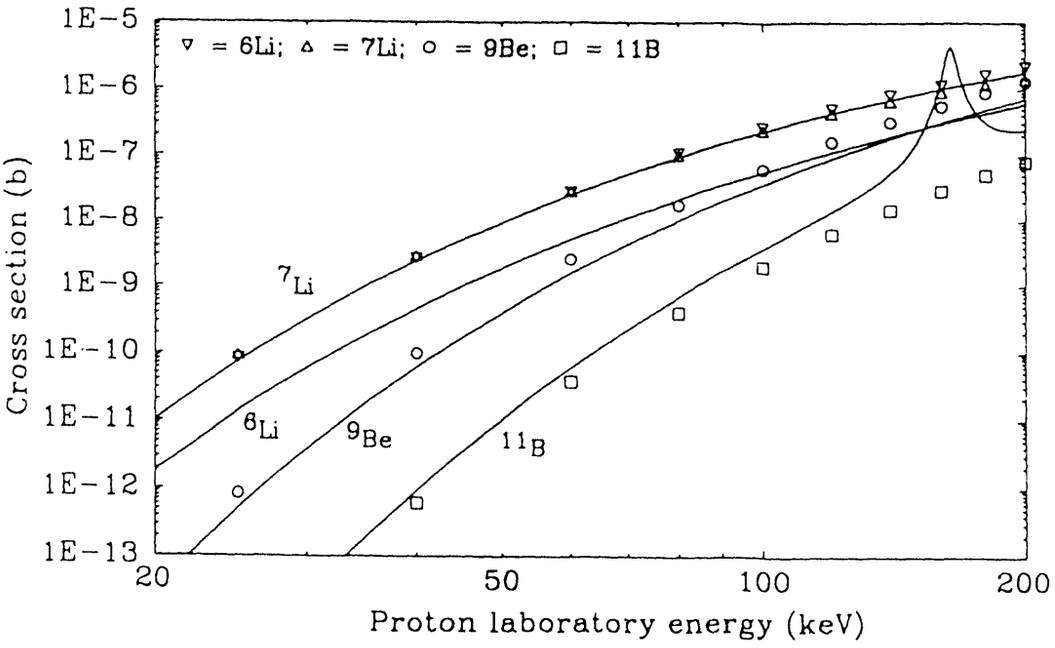

Fig. 1 Comparison of direct capture calculations (symbols) of the total cross sections for the ground state transitions and the experimental cross sections (solid lines).

B PUBLICATIONS AND REPORTS—October 1, 1990 to October 1, 1991

1. Published Articles

1. Nuclear Ground-State Correlations in the Relativistic Random-Phase Approximation, J.A. McNeil, C.E. Price and J.R. Shepard, Phys. Rev. **C 42** 2442 (1990)
2. Meson Exchange Current Corrections to Magnetic Moments in Quantum Hadrodynamics, T. Morse, C.E. Price and J.R. Shepard, Phys. Lett. **251B** 241 (1990)
3. Deformed Chiral Nucleons, C.E. Price and J.R. Shepard, Phys. Lett. **259B** 1 (1991)
4. Toward a Consistent RHA-RPA, J. R. Shepard, in *Proceedings of the Workshop: From Fundamental Fields to Nuclear Phenomena*, eds. J. A. McNeil and C. E. Price, (World Scientific, 1991)
5. *Proceedings of the Workshop: From Fundamental Fields to Nuclear Phenomena*, J. A. McNeil and C. E. Price, eds. (World Scientific, 1991)
6. Measurement of Spin Observables in the ^{28}Si$(\vec{p},\vec{p}')$ Reaction at 500 MeV and Comparison with Distorted-wave Impulse Approximation, E. Donohue, C. Glashausser, A. Sethi, J. Shepard, R. Fergerson, M. Franey, M. Gazzaly, K. Jones, J. McClelland, S. Nanda, and M. Plum, Phys. Rev. **C43** 213 (1991)

2. Articles Accepted or Submitted for Publication

1. Charge Density Differences Near ^{208}Pb in Quantum Hadro-Dynamics, R. J. Furnstahl and C. E. Price, accepted by Phys. Rev. **C**
2. Excitation of the 10.957 MeV 0^-;T=0 State in ^{16}O by 400 MeV Protons, J.D. King, D. Frekers, R. Abegg, R.E. Azuma, L. Buchmann, C. Chan, T.E. Drake, R. Helmer, K.P. Jackson, L. Lee, C.A. Miller, E. Rost, R. Sawafta, R. Schubank, S.S.M. Wong, S. Yen and X. Zhu, accepted by Phys. Rev. **C**
3. Complete Spin Transfer Measurements for Inelastic Polarized Proton Scattering from ^{12}C, X.Y. Chen, J.R. Shepard, M.R. Braunstein, T.A. Carey, K.W. Jones, J.B. McClelland, L. Rees, T.N. Tadeucci and N. Tanaka, accepted by Phys. Rev. **C**
4. Distorted Wave Born Approximation, P.D. Kunz and E. Rost, in *Computational Nuclear Physics*, J.A. Maruhn ed., Springer Verlag, Heidelberg, to be published 1991.
5. 0^+ and 2^+ Strengths in Pion Double Charge Exchange to Double Giant Dipole Resonances, J.M. O'Donnell, H.T. Fortune and E. Rost, submitted to Phys. Rev. **C**

3. Invited and Contributed Papers

1. Towards a Consistent RHA-RPA, J. A. Shepard, From Fundamental Fields to Nuclear Phenomena, Boulder Colorado, September 20-22 1990
2. Correlation Energy in QHD, J. A. McNeil, T. C. Ferrée, C. E. Price and J. R. Shepard, B.A.P.S. **36** 1269 (1991)

END

DATE FILMED

10/2/91